Journal of
Medicinal Chemistry

Article

Discovery of 3-oxabicyclo[4.1.0]heptane, a non-nitrogen containing morpholine isostere, and its application in novel inhibitors of the PI3K-AKT-mTOR pathway.

Heather Hobbs, Gianpaolo Bravi, Ian B. Campbell, Maire A. Convery, Hannah Davies, Graham Inglis, Sandeep Pal, Simon Peace, Joanna Redmond, and Declan Summers

J. Med. Chem., **Just Accepted Manuscript** • DOI: 10.1021/acs.jmedchem.9b00348 • Publication Date (Web): 08 Jul 2019

Just Accepted

is published by the American Chemical Society. 1155 Sixteenth Street N.W., Washington, DC 20036

Discovery of 3-oxabicyclo[4.1.0]heptane, a non-nitrogen containing morpholine isostere, and its application in novel inhibitors of the PI3K-AKT-mTOR pathway.

Heather Hobbs*, Gianpaolo Bravi[†], Ian Campbell, Maire Convery, Hannah Davies, Graham Inglis, Sandeep Pal, Simon Peace, Joanna Redmond & Declan Summers[ψ].

GlaxoSmithKline R&D, Gunnels Wood Road, Stevenage, SG1 2NY, U.K.

[†]Current affiliations: [†]Dotmatics, The Old Monastery, Windhill, Bishops Stortford, CM23 2ND.

[ψ]Costello Medical Consulting Ltd, Jupiter House 10, Cambridge, CB1 2JD.

Abstract

4-(Pyrimidin-4-yl)morpholines are privileged pharmacophores for PI3K and PIKKs inhibition by virtue of the morpholine oxygen both forming the key hydrogen bonding interaction and conveying selectivity over the broader kinome. Key to the morpholine utility as a kinase hinge binder is its ability to adopt a co-planar conformation with an adjacent aromatic core favoured by the morpholine nitrogen non-bonding pair of electrons interacting with the electron deficient pyrimidine π-system. Few selective morpholine replacements have been identified to date. Herein we describe the discovery of a potent non-nitrogen containing morpholine isostere, with the ability to mimic this conformation and its application in a potent selective dual inhibitor of mTORC1 and mTORC2 [**29b**].

Introduction

The phospoinositide 3-kinase kinase (PI3K)-AKT-mammalian target of rapamycin (mTOR) pathway has attracted much attention from the scientific community as a key regulator of diverse cellular processes including: growth; proliferation; metabolism; differentiation; autophagy; survival and cytoskeleton rearrangement[1]. The pathway is one of the most commonly dysregulated in cancer[2-4] and is also implicated in metabolic disorders and neurodegeneration[5-8]. Several ATP competitive and non-competitive pathway inhibitors are already in the clinic[9-11] and it is likely that much of the pharmaceutical industry is still active in this field[12-17].

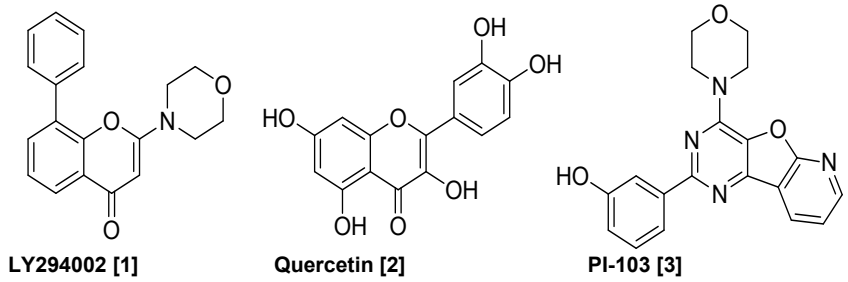

Figure 1: Structures of LY294002 **1**, Quercetin **2**, PI-103 **3**

Morpholine acts as the hinge binder in the very first reported synthetic inhibitor of the PI3Ks, LY294002 [**1**][18, 19] (**Figure 1**). The X-ray co-crystal structures of **1**, and structurally related Quercetin **[2]**, with porcine PI3Kγ were published in 2000 and highlight the key hydrogen bonding interaction between the morpholine oxygen of **1** and Val882 which mimics the N1 interaction of the natural substrate, ATP[20]. Subsequent crystal structures, including dual PI3K-mTOR inhibitor PI-103 **3** bound to mTOR[21] further support the key morpholine-hinge hydrogen bond hypothesis and highlight the co-planarity of the morpholine and adjacent ring systems when binding to the respective active sites.

4-(Pyrimidin-4-yl)morpholine [**A]** is a privileged pharmacophore for the PI3K-AKT-mTOR pathway[22-24] and is widely conserved across selective PI3K and PIKK inhibitors. Minimization of the dihedral angle CNcn (where C and N atoms belong to the aryl ring and the c and n atoms belonging to the aromatic ring) of 4-(Pyrimidin-4-yl)morpholine [**A]** using Density Functional Theory (DFT) and

6.31G** basis set in Jaguar[25] shows that the morpholine ring and the aryl ring are co-planar. This is due to stabilising electronic overlap between the nitrogen lone pair and the aryl ring (***Figure 2***).

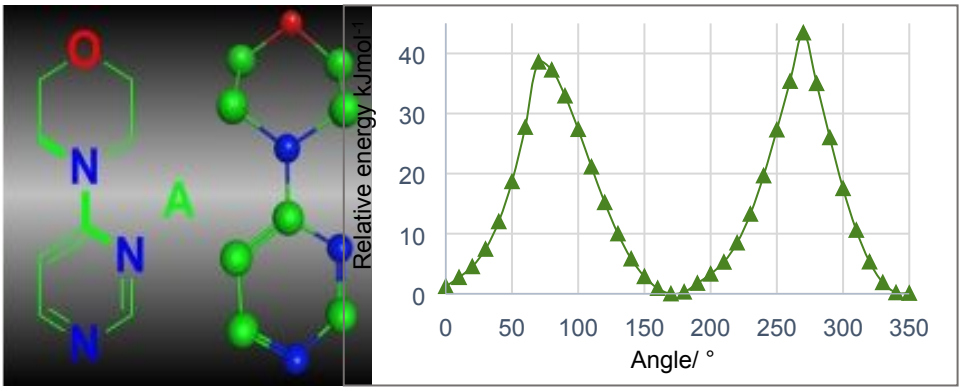

Figure 2: **(a)** Energy minimised structure of 4-(Pyrimidin-4-yl)morpholine **[A]** using DFT. **(b)** Energy scanning plot of CNcn dihedral bond angle of **A**

Kinase inhibitors described to date possessing a morpholine hinge binder have shown exclusive selectivity for the Lipid Kinases[26] and the adjacent electron deficient pyrimidine ring induces co-planarity, orientating the morpholine oxygen loan pair in the optimal vector for formation of the key hydrogen bonding interaction. Replacements for the morpholine ring are rare and limited largely to heteroaromatic rings or dihydropyran[27], both of which conserve the co-planar geometry. However the combination of multiple aromatic rings has significant implications for 'drug like' properties[28, 29] and simple, planar structures are often associated with poor physicochemical profiles and toxicity whilst increasing carbon bond saturation (Fsp^3), and structural complexity is correlated with improved solubility and success of compounds progressing into the clinic[30, 31]. The dihydropyran (DHP) hinge binder retains cross-kinome selectivity but has not been widely utilised in the literature, presumably due to its reduced Fsp^3 character, poor solubility profile and potential reactivity. Limited examples of the fully saturated tetrahydropyran (THP) exist in the literature[27] but despite retaining the key oxygen, the inability of the THP to adopt a low energy co-planar conformation means the THP analogues are invariably less active than their unsaturated or morpholine analogues due to the conformational energy penalty to form the key hydrogen bonding interaction.

Herein we report the discovery of a novel, stable, carbon linked saturated cyclic system with increased Fsp^3 and differentiated physicochemical profile with the potential to mimic the binding mode of

morpholine. Full comparative matched molecular pairs were prepared and described to give clear and complete understanding of changing factors.

Results and Discussion

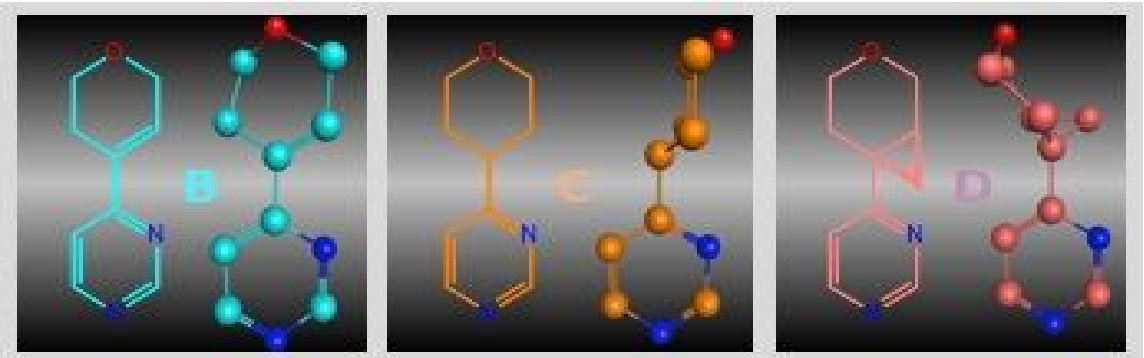

Figure 3: Dihydropyran pyrimidine **[B]**, Tetrahydropyran pyrimidine **[C]** & CPP pyrimidine **[D]** Energy minimised structures using MMFF94X forcefield in MOE

A brainstorm approach to novel alternative carbon-linked morpholine isosteres with improved Fsp^3 lead us to consider the potential for 3-oxabicyclo[4.1.0]heptane (cyclopropyl pyran or CPP) to adopt a co-planar conformation with a pyrimidine core given that cyclopropyl carbon-carbon bonds are known to form stabilising interactions with adjacent π-systems[32-34]. Energy minimization using molecular mechanics using MMFF94X force field in MOE[35] showed good structural overlap between morpholine pyrimidine **[A]** and dihydropyran (DHP) pyrimidine **[B]**, however tetrahydropyran (THP) pyrimidine **[C]** and 3-oxabicyclo[4.1.0]heptane pyrimidine **[D]** were both predicted to adopt preferred orthogonal geometries (**Figure 3**).

Similarly, investigation of the Cambridge crystallographic database also suggested that most cyclopropyl-aromatic combinations afford orthogonal geometry [e.g. CSD code ULIXIX]; however, the structures exemplified in the crystallography database are predominantly cyclopropyl-phenyl combinations. Prior to discarding this option, rigorous quantum mechanical calculations using Density Functional Theory (DFT) and 6.31G** basis set in Jaguar[25] were undertaken which predicted a *co-planar* conformation for CPP (D). (***Figure 4***).

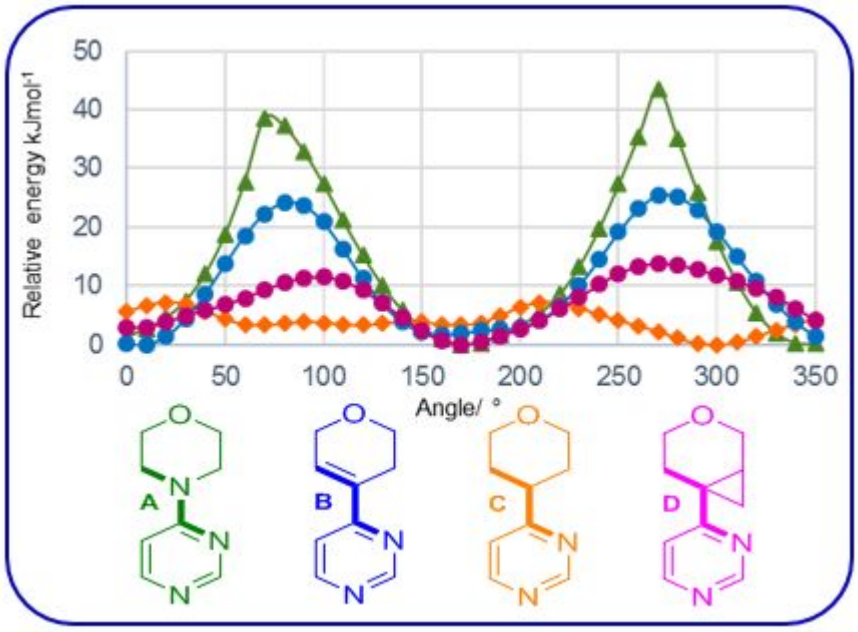

Figure 4: Dihedral scanning plots for various pyrimidine fragments using DFT/6-31G**

The data in **Table 1** supports the hypothesis documented in the literature[27] that the dihydropyran **[9]** is a reasonable replacement for the morpholine **[5]** and 3-S-methylmorpholine **[6]** across a range of common lipid and lipid-like kinases with only a slight loss in affinity. The tetrahydropyran **[11]** loses significant affinity, in line with the hypothesis that is can only form the key oxygen hydrogen bound by adopting a less energetically favourable conformation.

The CPP **[12]** is a chiral molecule and exists as two isomers **[12a]** (3-(4-((1*R*,6*S*)-1-methyl-3-oxabicyclo[4.1.0]heptan-6-yl)pyrimidin-2-yl)phenol) and **[12b]** (3-(4-((1*S*,6*R*)-1-methyl-3-oxabicyclo[4.1.0]heptan-6-yl)pyrimidin-2-yl)phenol).

The absolute stereochemistry of **12a** and **12b** are inferred from the small molecule crystal structure of **12b** (**Figure 5b,** see supporting information)[36] which has negative optical rotation. All subsequent. cyclopropyl pyrans reported here are assigned relative to **12b** by their optical rotation. Compounds with negative optical rotation are assumed 1*S*,6*R*

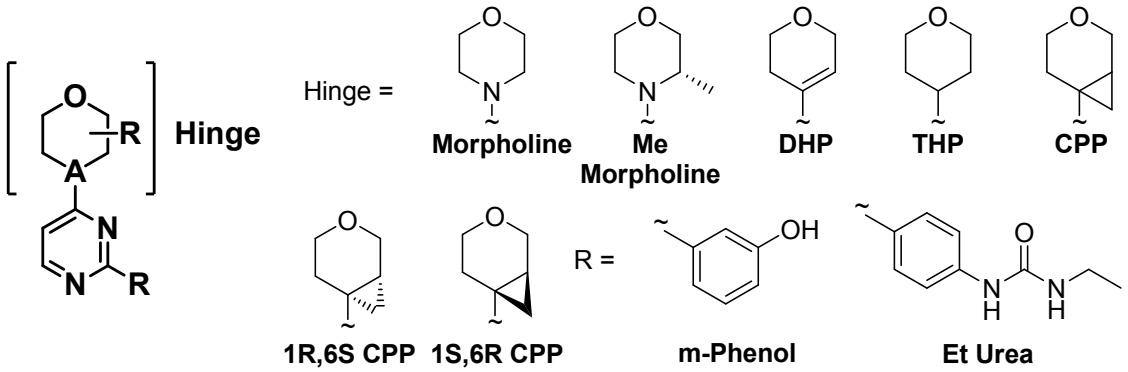

	Hinge	R	PI3Kα pIC_{50}[a]	PI3Kδ pIC_{50}[a]	mTOR pIC_{50}[a]	pAKT pIC_{50}[a]	Fsp^3	Chrom LogP[b]	Solubility (μg/mL)[c]
5	Morpholine	m-phenol	6.3	6.6	5.9	5.7	0.29	2.7	107
6	Me Morpholine		5.8	6.0	5.7	5.4	0.33	3.3	119
9	DHP		5.5	5.9	5.7	5. 5	0.2	3.6	113
11	THP		4.8	5.1	4.5	4.7	0.33	3.3	100
12	CPP		5.2	5.4	4.8	5.1	0.38	4.1	102
12a	1*R*,6*S* CPP		5.2	5.5	<3[d]	5.0	0.38	4.0	123
12b	1*S*,6*R* CPP		5.6	5.9	5.1	5.1	0.38	4.0	141
7	Morpholine	Et urea	4.9	5.0	6.5	5.4	0.35	2. 7	109
8	Me Morpholine		5.2	5.3	6.1	5.9	0.39	3.4	136
10	DHP		4.7	4.8	6	5.4	0.28	3.6	24
13	CPP		4.9	5.3	5.8	5.5	0.42	4	111
13a	1*R*,6*S* CPP		<4.5	4.6	5.5	5.5	0.42	3.9	127
13b	1*S*,6*R* CPP		4.6	4.6	6.1	5.7	0.42	3.9	125

Table 1: Biochemical assay data for tool compounds **5-13**

[a]Mean value of at least two repeat measurements per data point, (see supporting information for details). [b]Chrom LogP is the lipophilicity of the compound in its neutral state measured using reversed phase column chromatography (50 x 2 mm 3 μM Gemini NX C18, Phenomenex, UK) with fast acetonitrile gradient at starting mobile phase of pHs 2, 7.4 and 10.5. Chrom LogP values are derived directly from the gradient retention times by using a calibration line obtained for standard compounds. [c]kinetic solubility assay: 5μl of 10mM DMSO stock solution diluted to 100ul with pH7.4 phosphate buffered saline, equilibrated for 1 hour at room temperature and filtered through Millipore $Multiscreen_{HTS}$-PCF filter plates and quantified by Charged Aerosol Detector. [d]Data from high concentration screen (1 mmol initial concentration).

The PI3K and mTOR kinase affinities and cellular efficacy (pAKT) of the more potent 1*S*,6*R* CPP isomer **[12b]** are broadly similar to the dihydropyran **[9]** although less potent and with lower lipophilic ligand efficiency, due to its increased lipophilicity, than the 3*S*-methylmorpholine **[6]**, supporting the hypothesis that the 3-oxabicyclo[4.1.0]heptane motif can not only adopt a co-planar geometry with the adjacent pyrimidine ring but also is an active bioisostere for morpholine. The small molecule crystal structure of **12b** confirms co-planarity in the solid phase and the visible electron density in a low occupancy co-crystal structure of **12b** in PI3Kδ (**Figure 5c**, not deposited in PDB due to low occupancy, see supporting information) is consistent with a favourable low energy co-planar binding conformation and the ability of the CPP pyrimidine motif to sit close to the hinge in the active site.

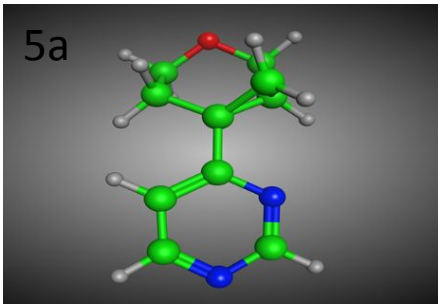

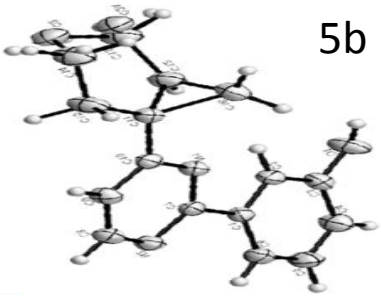

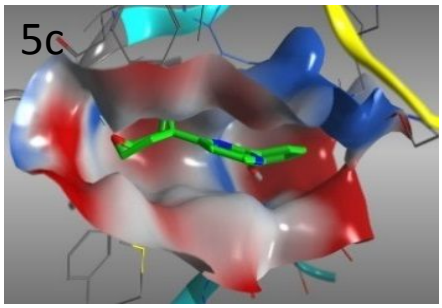

Figure 5a: QM predicted structure using DFT/6-31G**
5b: small molecule crystal structure of **12b** (CCDC 1864315 -See supplementary information)
5c: A potential binding mode of **12b** which is consistent with a low occupancy co-crystal structure in PI3Kδ (not deposited).

The emerging utility of mTOR inhibitors in diseases including a variety of cancers, thrombosis, fibrosis and diabetes[37-43], along with a marked prevalence for morpholine pyrimidines amongst the selective inhibitors in the literature lead us to apply our discovery to the development of potent selective 3-oxabicyclo[4.1.0]heptane (CPP) mTOR inhibitors. Compounds with a classical mTOR ethyl urea back pocket, such as **7**, **8** and **9** illustrate the 10-30-fold increased affinity of such molecules for the mTOR protein and improved selectivity over the closely structurally related PI3K isoforms. It is postulated that this increased affinity is due to the additional hydrogen bonding interactions between the urea moiety and the protein back pocket region. Gratifyingly this increased affinity for mTOR is conserved in the

CPP molecules, with **13b** demonstrating a full log unit of increased affinity over **12b** and similar potency to the morpholine **[7],** 3*S*-methylmorpholine **[8]** and dihydropyran **[10]** (with similar caveats to **12b** with respect to ligand efficiency and lipophilicity)**.** Furthermore, the selectivity of the 1*S*,6*R* analogue **[12b]** was improved by virtue of its reduced affinity for the class I PI3Ks. The CPP isomers **[13a** and **13b]**, with considerably increased lipophilicities over the morpholines **[7]** and **[8]**, might be expected to exhibit a dramatic drop in aqueous solubility. Whilst the data shown are kinetic solubility values, a significant drop in solubility is not apparent.

PI3KK research in the recent literature that caught our attention are the publications by AstraZeneca highlighting development of AZD3147 a dual mTORC1 mTORC2 inhibitor[44] and the closely related AZ20, a selective ATR inhibitor[45]. The authors postulate that increasing the 'non-planarity' in the hinge region by incorporation of the 3(S)-methylmorpholine has a positive impact on cellular efficacy and solubility due to disruption of hydrogen bonding networks, disruption of the crystal packing and an increased twist between the morpholine and pyrimidine rings. Disrupting planarity by alkylation of the methylene linker also had a positive impact on cellular potency but results in a significant increase lipophilicity. We were interested in the impact of the CPP in this series and the interplay between potency, lipophilicity, hydrogen bonding and solubility. To this end compounds **14, 15, 21, 22a, 22b, , 23a** and **23b** were synthesised (**Scheme 2 and 4**) as benchmarks for us to assess the impact of our CPP replacements in the sulphone series and are not included in our subsequent selectivity analysis as they incorporate a classical non-selective kinase back pocket, however these compounds confirm the general utility of the CPP replacement.

Whilst 1*S*,6*R* CPP **16b** shows a significant 5-fold drop in affinity over the 3S-methylmorpholine **[14]**, their cellular efficacies (as determined by pAKT pIC_{50}s: 5.5 vs 5.6) are almost identical, supporting hypothesis of a positive impact of increasing non-planarity (or Fsp3). It should be noted that the CPP isomers are also more lipophilic than the 3*S*-methylmorpholine (3.66 vs 3.33 respectively) and this increased lipophilicity will also have a positive effect on permeability (also true for the 3*S*-methylmorpholine vs morpholine matched pairs), however the increased lipophilicity should logically have a negative impact on aqueous solubility

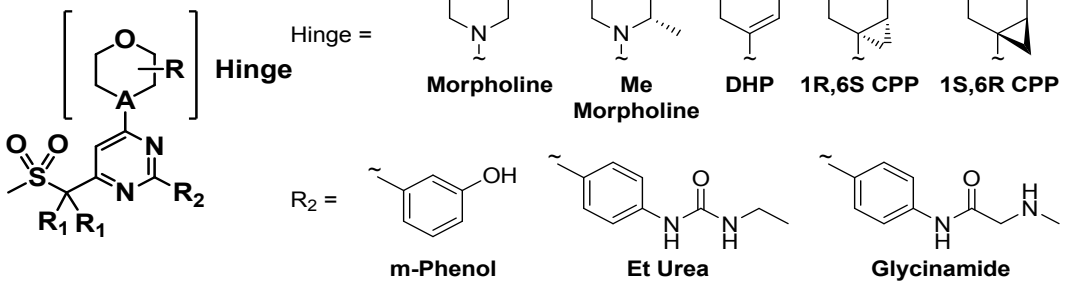

	Hinge	R1	R2	mTOR pIC_{50}[a]	pAKT pIC_{50}[a]	PI3Kα pIC_{50}[a]	PI3Kδ pIC_{50}[a]	Fsp^3	Chrom LogP[b]	Solubility (μg/mL)[c]
14	Me Morpholine	H	m-Phenol	6.7	5.6	6.0	6.0	0.41	3.3	113
21	DHP			6.4	6.1	5.2	5.8	0.29	3.3	27
22a	1*R*,6*S* CPP			5.9	5.3	5.1	5.4	0.44	3.7	145
22b	1*S*,6*R* CPP			5.8	5.5	4.7	4.8	0.44	3.7	75
15	Me Morpholine	Me		5.7	5.9	5.5	5.5	0.47	4.4	121
23a	1*R*,6*S* CPP			<5.4[d]	5.3	5.0	5.1	0.5	4.8	148
23b	1*S*,6*R* CPP			5.5	5.9	4.8	5.0	0.5	4.8	135
18	Morpholine	H	Et Urea	7.3	5.9	5.4	4.7	0.42	2.7	84
16	Me Morpholine			7,1	6.5	4.8	4.7	0.45	3.2	212
24a	1*R*,6*S* CPP			6.1	5.8	<4.5	4.6	0.48	3.6	77
24b	1*S*,6*R* CPP			7	6.3	<4.5	5.1	0.48	3.6	96
17	Me Morpholine	Me		7.3	7.3	5.1	5.1	0.5	4.4	130
25a	1*R*,6*S* CPP			6.6	6.8	4.6	4.8	0.52	4.7	78
25b	1*S*,6*R* CPP			6.9	7.2	<4.5	4.6	0.52	4.7	74
19	Me Morpholine	H	glycin-amide	7.7	6.3	4.6	4.9	0.45	2.6	90
26a	1*R*,6*S* CPP			7.1	5.9	<4.5	4.8	0.48	3.1	167
26b	1*S*,6*R* CPP			7.4	6.1	<4.5	<4.5	0.48	3.1	158
20	Me Morpholine	Me		8.0	7.3	4.8	5.8	0.5	4.1	198
27a	1*R*,6*S* CPP			7.3	6.8	4.6	5.9	0.52	4.3	257

27b	1*S*,6*R* CPP	——	7.6	7.0	<4.5	4.9	0.52	4.3	217

Table 2: Biochemical assay data for tool compounds **14-27**

[a]Mean value of at least two repeat measurements per data point. [b]Chrom LogP is the lipophilicity of the compound in its neutral state measured using reversed phase column chromatography (50 x 2 mm 3 µM Gemini NX C18, Phenomenex, UK) with fast acetonitrile gradient at starting mobile phase of pHs 2, 7.4 and 10.5. Chrom LogP values are derived directly from the gradient retention times by using a calibration line obtained for standard compounds. [c]kinetic solubility assay: 5µl of 10mM DMSO stock solution diluted to 100ul with pH7.4 phosphate buffered saline, equilibrated for 1 hour at room temperature and filtered through Millipore Multiscreen$_{HTS}$-PCF filter plates and quantified by Charged Aerosol Detector. [d]Compound **23a** tested inactive on two test occasions and positive on two test occasions (pIC_{50} 7.0 & 7.2), considering the other matched pair data we suspect that the active data points are due to a technical error.

which is not consistently apparent in our data. On average the CPP substituent solubility is broadly similar to the 3*S*-methylmorpholine which in AstraZeneca's hands were routinely 3-fold more soluble than the parent morpholines.

Compounds **16** to **20** and **24** to **27** incorporating mTOR selective back pockets show the 1*S*,6*R* CPPs **[24b 25b, 26b** and **27b]** and are broadly equipotent with their morpholine **[18]** and 3*S*-methylmorpholine analogues **[16, 17, 19** and **20]** but marginally more selective against the PI3K isoforms **(Figure 6a)**. Whereas the parent morpholine **[18]** shows limited cellular efficacy, the CPP analogues **[24b** and **25b]** are equiefficacious with the 3*S*-methylmorpholines **[16** and **17]**. It should be noted that compounds **22a** and **22b** do not appear to follow the general trend of the 1*S*,6*R* isomer **[22b]** being the more potent. In this matched pair the isomers are broadly equipotent. Our only explanation for this is a subtle change in binding pose facilitated by the small and non-selective phenol back pocket.

In line with AstraZeneca's findings, increasing the lipophilicity sulphone linker region with the dimethylated analogues resulted in increased cellular efficacy relative to the parent methylenes **[17** vs **16** and **20** vs **19]**, which is evident in the 1*S*,6*R* CCP methylmorpholine matched pairs as a lower average drop off from mTOR to pAKT pIC50's. A preliminary analysis of the effect of the CPP on aqueous solubility suggests a variable effect that is broadly positive in the polar m-phenol and glycinamide back pockets whereas with the highly planar urea back pocket the negative effect of increased lipophilicity dominates.

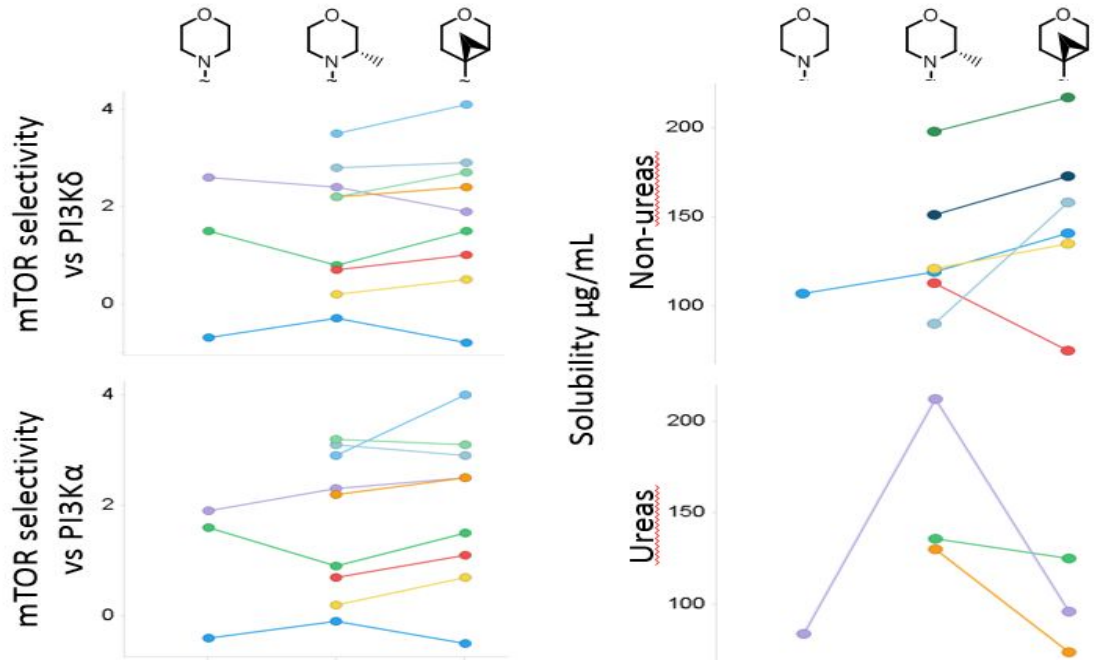

Figure 6: MMP comparisons of morpholine, 3*S*-methylmorpholine and 1*S*,6*R* CPP analogues

Finally, we synthesised one of the more potent analogues from the AstraZeneca paper[37] alongside the two CPP analogues (**Scheme 6**). Compound **28** was synthesised as described in the literature using the modified palladium cross coupling conditions used as standard in our labs.

1-(2-hydroxyethyl)-3-(4-(4-((1*S*,6*R*)-1-methyl-3-oxabicyclo[4.1.0]heptan-6-yl)-6-(2-(methyl-sulfonyl)propan-2-yl)pyrimidin-2-yl)phenyl)thiourea **29b** is a single-digit nanomolar, selective mTOR inhibitor with excellent selectivity over closely related kinases. **29b** compares favourably to the literature compound **28** with respect to mTOR affinity, efficacy, PI3K isoform selectivity and aqueous solubility.

To examine the potential of the CPP morpholine replacement to have an impact in a clinical setting we further profiled compounds **8**, **13a**, **13b**, **28** & **29b**.

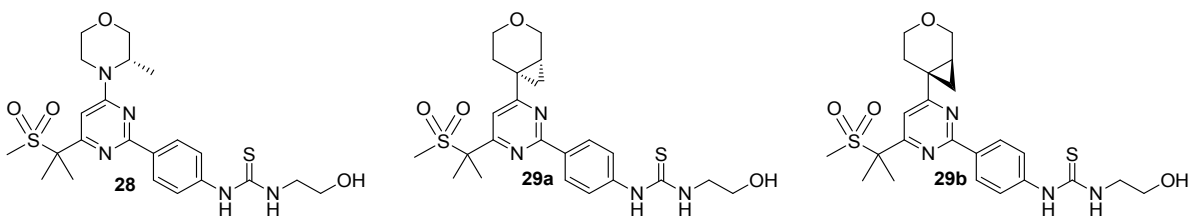

	mTOR pIC_{50}[a]	pAKT pIC_{50}[a]	PI3Kα pIC_{50}[a]	PI3Kδ pIC_{50}[a]	Fsp^3	Chrom LogP[b]	Solubility (μg/mL)[c]
28	8.4	7.4	5.5	4.9	0.5	3.6	151
29a	8.2	7.1	5.1	4.6	0.52	3.9	145
29b	8.6	7.5	4.6	4.5	0.52	3.9	173

Table 3: Biochemical assay data for nanomolar mTOR inhibitors 28-29

[a]Mean value of at least two repeat measurements per data point. [b]Chrom LogP is the lipophilicity of the compound in its neutral state measured using reversed phase column chromatography (50 x 2 mm 3 μM Gemini NX C18, Phenomenex, UK) with fast acetonitrile gradient at starting mobile phase of pHs 2, 7.4 and 10.5. Chrom LogP values are derived directly from the gradient retention times by using a calibration line obtained for standard compounds. [c]kinetic solubility assay: 5μl of 10mM DMSO stock solution diluted to 100ul with pH7.4 phosphate buffered saline, equilibrated for 1 hour at room temperature and filtered through Millipore $Multiscreen_{HTS}$-PCF filter plates and quantified by Charged Aerosol Detector

The metabolic stability of matched pair compounds were assessed in human and rat microsomes to determine the relative stability of the CPP with the m-phenol **[13a** & **13b]** and the urea back pockets **[29b]** compared to the 3*S*-methylmorpholine **[8** and **28]**. All three m-phenol compounds showed moderate clearance profiles in human whereas in rat the CPP containing compounds were readily turned over. Compounds **28** and **29b** were assessed in both human and rat microsomes and hepatocytes. Compound **28** was found to be a relatively low clearance compound, although it is moderately cleared in rat hepatocytes. Compound **29b** however is rapidly eliminated in both species in line with its increased lipophilicity. This data suggests no measurable difference between the two CPP isomers and but a specific metabolic liability with the cyclopropyl pyran substituent in rats.

As an exemplar of the CPP series, compound **27a** was profiled across a range of 17 kinases closely related to mTOR (ATM, ATR, CSNK2A1, CSNK2A2, PIK3C2A, PIK3C2B, PIK3C3, PIK3CA, PIK3CB, PIK3CD, PIK3CG, PIK3R4, PI4KA, PI4KB, PI4K2B, PRKDC [DNAPK], RIOK2) in a chemoproteomics kinobead screening assay and showed greater than x100 fold selectivity against each with the exception of PIK3CB (x55 fold selectivity). Other cyclopropylpyrans, not reported here, showed marked ATM and ATR potency.

	Hinge	Back Pocket	rat Cl_{int} mL/min/g microsomes	human Cl_{int} mL/min/g microsomes	rat Cl_{int} mL/min/g hepatocytes	human Cl_{int} mL/min/g hepatocytes
8	Me Morpholine	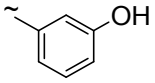	2.0	1.2		
13a	1*R*,6*S* CPP		16.7	1.4		
13b	1*S*,6*R* CPP		13.6	1.5		
28	Me Morpholine	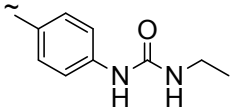	0.8	0.9	2.8	0.9
29b	1*S*,6*R* CPP		1.4	3.1	13.0	5.1

Table 4: metabolic stability data for morpholine and CPP matched molecular pairs

Chemistry

Compounds **5** – **8** were synthesised by precedented chemistry[44] according to the route outlined in Scheme 1a. The reaction of morpholine or 3*S*-methylmorpholine with 2,4-dichloropyrimidine and Hunig's base proceeds selectively at room temperature to give intermediates **A** and **B** in good yield. Installation of the non-selective m-phenol and mTOR selective back pockets via Suzuki-Miyaura cross coupling[46, 47] with the relevant pinacol boronic esters afforded tool compounds **5, 6, 7** and **8** in good yields.

Similarly, Palladium mediated cross coupling furnished dihydropyran compounds intermediate **C** and subsequently **9** and **10** in good yields. Compound **9** was reduced with hydrogen over a palladium on carbon catalyst to afford the tetrahydropyran **11**. The synthesis of **12** and **13** were affected by a Johnson-Corey-Chaykovski cyclopropanation of **9** and **10** respectively in moderate yields. Interestingly Simmons-Smith cyclopropanation afforded none of the desired products. Simmons-Smith cyclopropanation is effective with electron rich systems, compounds **9** and **10** are both electron deficient by virtue of the neighbouring pyrimidine hence favouring the Johnson-Corey-Chaykovski cyclopropanation. Compounds **12** and **13** were subsequently separated into their single enantiomers **12a, 12b, 13a** and **13b** by chiral SFC.

Scheme 1a: General Synthesis of Parent Morpholines **5**, **6**, **7** and **8**

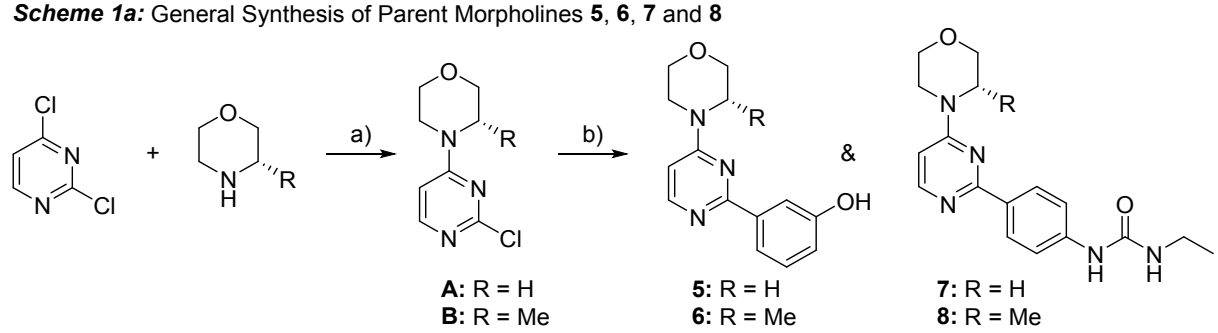

Scheme 1b: General Synthesis of Dihydropyrans **9** & **10**, Terahydropyran **11** and Cyclopropylpyrans **12** and **13**

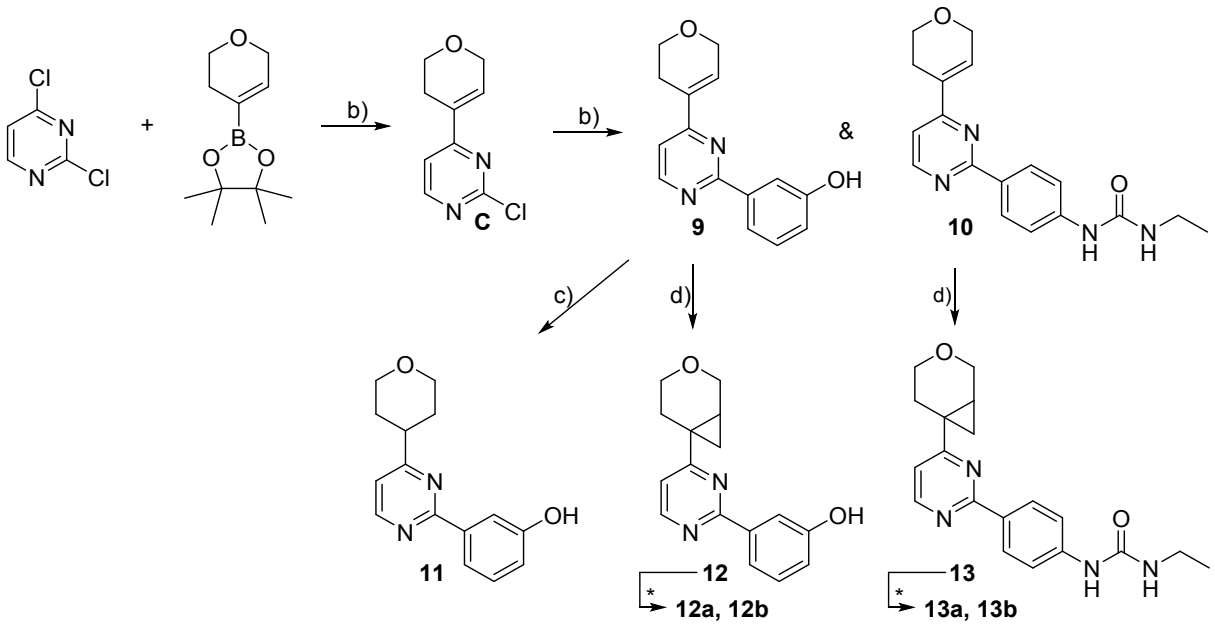

Reagents: a) (*S*)-3-methylmorpholine, DIPEA rt. b) Borolane, $PdCl_2(dppf)$, K_2CO_3, isopropanol:water 5:1, 110°C, 2h. c) Pd/C 5%, CH_3CO_2H, HCl/Zn 50°C, 4h. * Chiral SFC d) Me_3SO, NaH, DMSO, 65°C, 4h.

The synthesis of 3-[4-(methanesulfonylmethyl)- and 3-[4-(2-methanesulfonylpropan-2-yl)- 6-[(3*S*)-3-methylmorpholin-4-yl]pyrimidines is highlighted in **Scheme 2** utilising literature intermediates **D** and **E**[44] and palladium cross coupling conditions favoured in-house to furnish the *m*-phenols **14** and **15**, *p*-phenyl ethyl ureas **16** and **17** and *p*-phenyl glycinamides **19** and **20**. 1-ethyl-3-(4-(4-((methylsulfonyl)methyl)-6-morpholinopyrimidin-2-yl)phenyl)urea (**18**) was synthesised as described as previously[44] using the modified palladium cross coupling conditions used as standard in our labs.

Scheme 2: General Synthesis of Compounds **14** to **20**

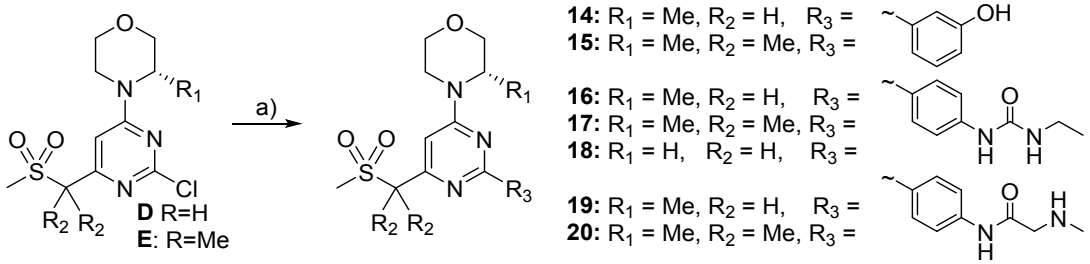

Reagents: a) Borolane, $PdCl_2(dppf)$, K_2CO_3, isopropanol:water 5:1, 110°C, 2h. .

The synthesis of 3-oxabicyclo[4.1.0]heptanes **22**, **23**, **24**, **25**, **26** and **27** was improved over the two-step synthesis of tool compounds **12** and **13** by the initial synthesis of the 3-oxabicyclo[4.1.0]heptane pinacol boronic ester, intermediate **F** and subsequent activation by conversion to the potassium 3-oxabicyclo[4.1.0]heptan-6-yltrifluoroborate intermediate **G** (**Scheme 3**). Palladium mediated cross couplings with intermediate **G** produced consistently better yields than coupling directly with intermediate **F**.

Scheme 3: Synthesis of **Intermediate G**

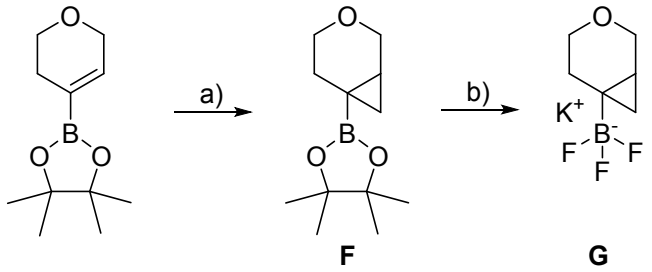

Reagents: a) Et_2Zn, CH_2ClI, fluorobenzene, -5°C, multiple additions, rt 16h.
b) KF/H_2O, MeCN/MeOH, 2(2*R*,3*R*)-2,3-dihydroxysuccinic acid, THF rt.

The synthesis of 6-((methylsulfonyl)methyl)pyrimidine and 6-(2-(methylsulfonyl)propan-2-yl)pyrimidine compounds **21** to **27**, highlighted in Scheme **4**, proceeds via the synthesis of known intermediate **H**[44]. Suzuki-Miyaura cross-coupling chemistry, already described, furnished intermediate **I** and conditions optimised specifically for the coupling of intermediate **G** were utilised to deliver intermediate **J** in a single coupling step from the aryl chloride. Intermediate **I** was coupled with 3-(4,4,5,5-tetramethyl-1,3,2-dioxaborolan-2-yl)phenol to afford compound **21**.

Intermediate **J** was reacted with methyl iodide in the presence of sodium *tert*-butoxide to give the dimethylated intermediate **K.** Having established that the separate enantiomers were stable to the palladium mediated cross-coupling conditions intermediates **J** and **K** were separated by chiral SFC to

afford intermediates **L, M, N** and **O** prior to palladium-cross coupling to furnish compounds **22, 23**, **24, 25, 26** and **27**.

Scheme 4: General Synthesis of Compounds **21 to 27**

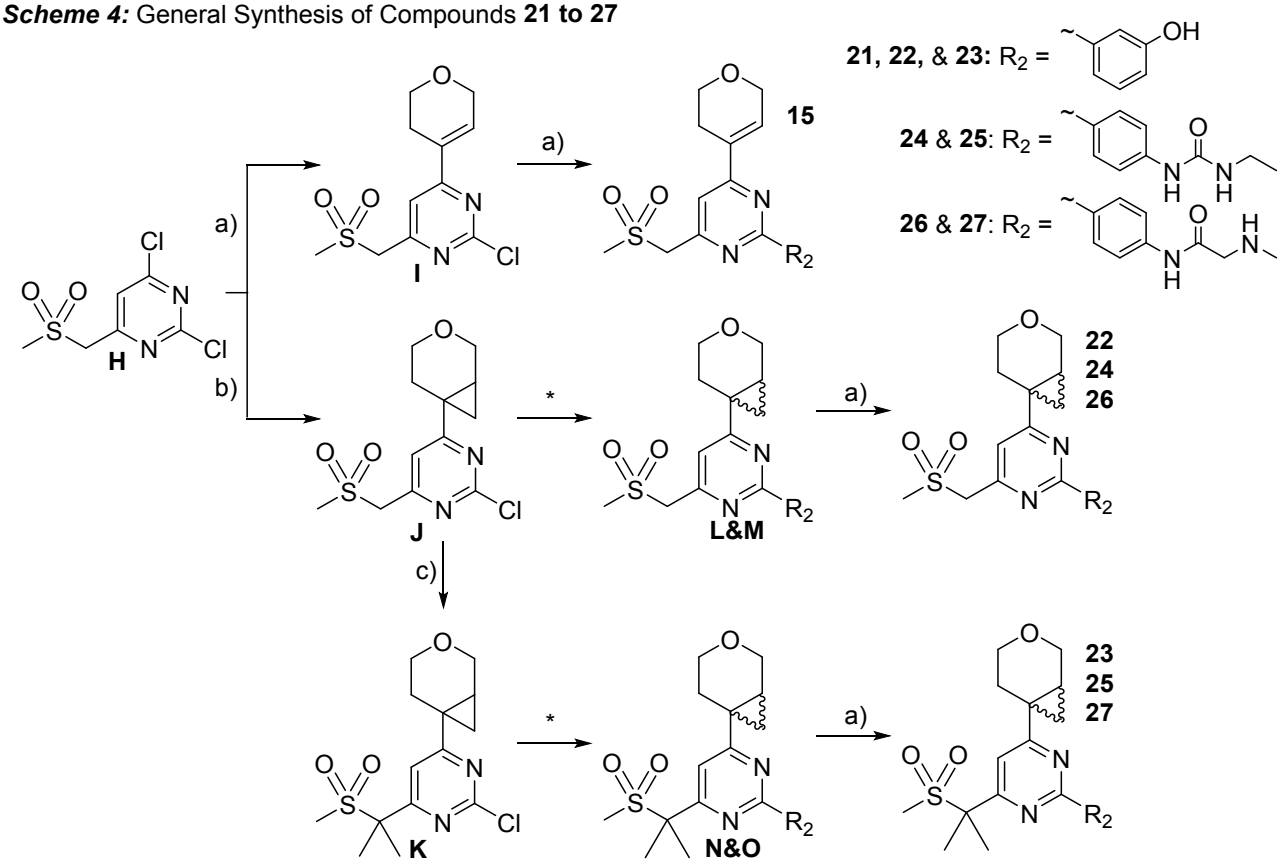

Reagents: a) Borolane, $PdCl_2(dppf)$, K_2CO_3, isopropanol:water 5:1, 110°C, 2h. b) **Intermediate G**, $PdCl_2$, Cs_2CO_3, toluene:water 10:1, 110°C, 15h. * Chiral separation

Scheme 5 Synthesis of Compounds **29a** and **29b**

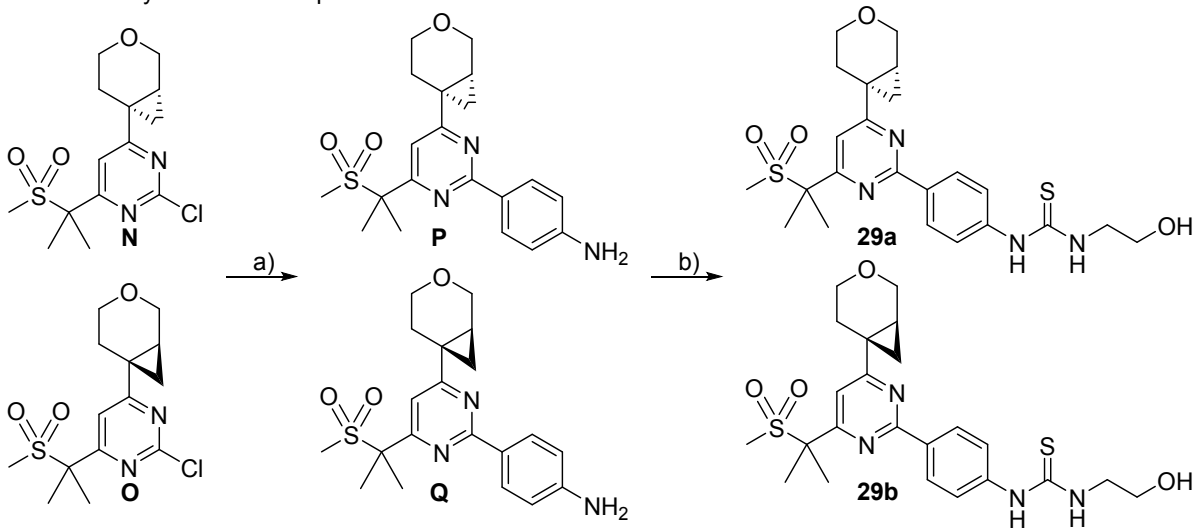

Reagents: a) Borolane, $PdCl_2(dppf)$, K_2CO_3, isopropanol:water 5:1, 110°C, 2h. b) 1,1'-thiocarbonyldiimidazole, DCM rt 4h then ethanolamine 0°C to rt 18h.

The synthesis of sub nanomolar mTOR inhibitors **29a** and **29b** is described in **Scheme 5**. Intermediates **N** and **O** were coupled using our standard palladium cross-coupling conditions to afford intermediates **P** and **Q** in moderate yields. Conversion of the aniline intermediates to the thioureas proceeded via a two-step, one pot process involving initial formation of the thioisocyanates with di(imidazol-1-yl)methanethione followed by addition of ethanolamine to afford **29a** and **29b** in excellent yields.

Conclusion

Herein we have outlined the discovery of 3-oxabicyclo[4.1.0]heptane and demonstrated the use of in-depth quantum mechanical calculations to predict the low energy co-planar conformation of the cyclopropyl pyran attached to a pyrimidine ring. The anticipated co-planar geometry was confirmed through a small molecule crystal structure of compound **12b** and further supported by maintenance of potency compared with morpholine analogues. A preliminary co-crystal structure of **12b** in PI3Kδ supported our hypothesis of co-planarity in the active site and is consistent with maintenance of the key hydrogen bonding interaction, found in **PI-103,** that is common to all known morpholine based PI3K and PIKK inhibitors. We have performed a very thorough matched molecular pair analysis and provided a substantial data set illustrating that the incorporation of this novel moiety has increased FSp^3 character whilst removing an embedded aniline and therefore reducing the risk of genotoxic metabolites being formed *in vivo* without a detrimental effect on solubility.

Following clear selectivity signals from our dataset we subsequently applied our discovery to a published series of selective mTOR inhibitors and shown that the cyclopropyl pyran analogue **29b** retains mTOR affinity and cellular efficacy with an improved selectivity over the class I PI3K isoforms and similar solubility profile when compared to the published 3*S*-methylmorpholine analogue **28**.

The tractability of the single enantiomers of the CPP remains a synthetic challenge and efforts towards a homochiral synthesis in house have, to date, proved unsuccessful with all single enantiomers described herein being isolated by chiral chromatography. In addition, the disconnect between the metabolic profile of the CPPs in rat and human has the potential to cause significant problems in obtaining rodent safety cover and predicting human PK and dose using traditional allometric scaling techniques;

however, such problems could be overcome using modern techniques such as PB/PK modelling. The CPP matched molecular pairs have failed to address the metabolic clearance typically associated with the 3*S*-methylmorpholine with consistently elevated clearance profiles, in good agreement with the increased lipophilicity of the CPP substituent.

The replacement of N-aryl saturated heterocycles with fused cyclopropanes extends well beyond the lipid kinase field and, in principle, provides an alternative approach to control conformation besides the use of an aryl nitrogen. A full investigation into the steric and electronic requirements to obtain co-planar geometry has been undertaken and will be reported in due course[36].

Experimental Section

General.

All solvents and reagents, unless otherwise stated, were commercially available from regular suppliers such as Sigma-Aldrich and Fluorochem and were used as purchased without further purification. When necessary organic phases were filtered through ISOLUTE® phase separator hydrophobic frits, which contain a membrane which is selectively permeable to organic solutions to remove traces of water. Intermediates were purified by flash column chromatography on Redisep® Rf flash columns using an Isco Combi Flash Rf+ companion or similar eluting with increasing percentages of ethyl acetate in cyclohexane. Compounds for biological testing were purified either by Mass Directed HPLC on C18 5um 30x150mM XSelect CSH columns using decreasingly polar mixtures of acetonitrile in water with either a formic acid or ammonium carbonate modifier or by preparative HPLC on a Reveleris® prep using C18 5um 30x100mM Waters Xbridge columns using decreasingly polar mixtures of acetonitrile in water with an ammonium carbonate modifier or C18 5um 30x100mM Waters Sunfire columns using decreasingly polar mixtures of acetonitrile in water with a formic acid or modifier. The purity of samples was assessed by NMR and HPLC and mass spectroscopy and are consistent with the proposed structures. The purity of compounds for biological testing were assessed by NMR, HPLC and mass spectroscopy techniques and were ≥ 95% unless otherwise quoted. LCMS analysis was carried out on a Waters Acquity UPLC instrument equipped with a BEH column (50 mm x 2.1 mm, 1.7 µm packing diameter) and Waters Micromass ZQ MS using alternate-scan positive and negative electrospray.

Analytes were detected as a summed UV wavelength of 210–350 nm. Samples were eluted with using decreasingly polar mixtures of acetonitrile in water with either a formic acid or ammonium carbonate modifier. Electrospray mass spectral data was obtained using a Waters ZQ/LC/mass spectrometer. Proton and carbon nuclear magnetic resonance (^{1}H NMR and ^{13}C NMR) spectra were recorded in deuterated solvents at ambient temperature on a Bruker AVI (400 MHz), or Bruker AVII+ (600 MHz) spectrometer (with cryoprobe). Chemical shifts δ are reported in parts per million (ppm) relative to tetramethylsilane and are internally referenced to the residual solvent peak. Coupling constants (*J*) are given in hertz to the nearest 0.1 Hz. The following abbreviations have been used; s, singlet; d, doublet; t, triplet; q quartet; br, broad; and m, multiplet. High-resolution mass spectra were recorded on a Waters XEVO G2-XS quadrupole time-of-flight mass spectrometer, with analytes separated on an Acquity UPLC CSH C_{18} column (100mm x 2.1mm, 1.7µm packing diameter). LC conditions were 0.8 mL/min flow rate, 50 °C, injection volume 0.2 µL, using a gradient elution with (A) H_2O containing 0.1% (v/v) formic acid and (B) acetonitrile containing 0.1% (v/v) formic acid. Gradient conditions were initially 3% B, increasing linearly to 100% B over 8.5 min, remaining at 100% B for 0.5 min then decreasing linearly to 3% B over 0.5 min followed by an equilibration period of 0.5 min prior to the next injection.

General Method A

The appropriate chloropyrimidine or dichloropyrimidine (1 equiv.) was treated with the appropriate 4,4,5,5-tetramethyl-1,3,2-dioxaborolane (0.8 - 1.2 equiv.), $PdCl_2$(dppf) (0.08 equiv.) and potassium carbonate (2 equiv.) and the mixture suspended in degassed Isopropanol : Water 5 : 1. The reaction mixture was bubbled through with nitrogen for 1 minute prior to heating at 110 °C for 2 h. The reaction mixture was filtered through celite and eluted with EtOAc. The eluent was washed with water, filtered through a hydrophobic frit and concentrated by blow down. Intermediate compounds were purified by normal phase column chromatography, final compounds were purified by mass directed HPLC.

General Method B

Relevant 2-chloro-pyrimidine (1 equiv.) was treated with tert-butyl methyl(2-oxo-2-((4-(4,4,5,5-tetramethyl-1,3,2-dioxaborolan-2-yl)phenyl)amino)ethyl)carbamate (1.2 equiv.), $PdCl_2$(dppf) (0.08

equiv.) and potassium carbonate (2 equiv.) and suspended in degassed Isopropanol : Water 5 : 1. The reaction mixture was bubbled through with nitrogen for 1 minute prior to heating at 110 °C for 2 h. The reaction mixture was filtered through celite and eluted with EtOAc. The eluent was washed with water, filtered through a hydrophobic frit and concentrated by blow down. The sample was resuspended in DCM and treated with TFA (~10 equiv.) and allowed to stand for 1 h prior to concentration by low down and purification by mass directed HPLC.

General Method C

Sodium hydride (2 equiv.) was treated with trimethyloxosulfonium chloride (2 equiv.) under a nitrogen atmosphere. Anhydrous DMSO (2 mL/mmol) was added dropwise and the reaction mixture stirred for 20 min. A solution of relevant dihydro-2H-pyran-4-yl)pyrimidine (1 equiv.) in anhydrous DMSO (2 mL/mmol) was added and the reaction mixture stirred at 65 °C for 4 h. The reaction mixture was partitioned between EtOAc and water and the aqueous phase extracted three times with EtOAc. The combined organic phase was concentrated *in vacuo* and purified by column chromatography and recrystallisation from toluene.

General Method D

A solution of relevant aniline (1 equiv.) in dichloromethane at 0 °C was treated portion wise with 1,1'-thiocarbonyldiimidazole (2 equiv.) and the mixture was stirred at ambient temperature for 4 h. The mixture was re-cooled to 0 °C and ethanolamine (10 equiv.) was added. The mixture was stirred at ambient temperature for 18 h. The reaction mixture was concentrated *in vacuo* and the residue purified by Mass Directed HPLC.

4-(2-Chloropyrimidin-4-yl)morpholine (Intermediate A)

To a clear, colourless solution of morpholine (0.871 mL, 10.00 mmol) and DIPEA (3.49 mL, 20.00 mmol) in anhydrous N,N-dimethylformamide (DMF) (13 mL), was added 2,4-dichloropyrimidine (1.490 g, 10 mmol) dropwise and the resulting colourless solution was stirred at 20 °C for 1 h prior to concentration *in vacuo*. The crude product was purified by column chromatography to afford 4-(2-

chloropyrimidin-4-yl)morpholine (1.401 g, 7.02 mmol, 70% yield) as an amorphous white solid. ^{1}H NMR (400 MHz, $CDCl_3$): δ ppm 8.07 (d, *J* = 6.06 Hz, 1H), 6.39 (d, *J* = 6.06 Hz, 1H), 3.74-3.82 (m, 4H), 3.62- 3.67 (m, 4H); ESI (m/z): $[M+H]^+$ = 200

(3*S*)-4-(2-Chloropyrimidin-4-yl)-3-methylmorpholine (Intermediate B)

A suspension of 2,4-dichloropyrimidine (500 mg, 3.36 mmol) in acetonitrile (6.7 mL) in a microwave vial was treated with DIPEA (1759 µl, 10.07 mmol) and (*S*)-3-methylmorpholine (381 µl, 3.36 mmol). The vial was sealed and stirred at ambient temperature for 19.5 h prior to addition of further (*S*)-3-methylmorpholine (38.1 µl, 0.336 mmol). The reaction mixture was stirred at ambient temperature for a further 2 h. The reaction mixture was partitioned between EtOAc (50 mL) and water (50 mL). The aqueous phase was extracted with further EtOAc (2 x 20 mL) and the combined organic phase was filtered through a hydrophobic frit and concentrated *in vacuo*. The residue was purified by column chromatography to afford (3*S*)-4-(2-chloropyrimidin-4-yl)-3-methylmorpholine (483 mg, 67% yield). ^{1}H NMR (600 MHz, DMSO-d_6): δ ppm 1.19 (d, *J* = 6.8 Hz, 3 H) 3.16 (td, *J* = 12.9, 3.9 Hz, 1 H) 3.42 (td, *J* = 11.9, 3.1 Hz, 1 H) 3.57 (dd, *J* = 11.6, 3.2 Hz, 1 H) 3.70 (d, *J* = 11.6 Hz, 1 H) 3.92 (dd, *J* = 11.6, 3.9 Hz, 1 H) 3.98 (br d, *J* = 13.0Hz, 1 H) 4.33 (br s, 1 H) 6.79 (d, *J* = 6.2 Hz, 1 H) 8.10 (d, *J* = 6.2 Hz, 1 H); ESI (m/z): $[M+H]^+$ = 214

2-Chloro-4-(3,6-dihydro-2H-pyran-4-yl)pyrimidine (Intermediate C)

From General Method A

Yield 6.4%. ^{1}H NMR (400 MHz, $CDCl_3$) δ ppm 8.57 (d, *J* = 5.14 Hz, 1H), 7.28 (d, *J* = 5.14 Hz, 1H), 7.26 (d, *J* = 5.14 Hz, 1H), 7.10 (m, 1H), 4.42 (q, *J* = 2.93 Hz, 2H), 3.95 (t, *J* = 5.38 Hz, 2H), 2.59 (m, 2H) ; ESI (m/z): $[M+H]^+$ = 197

4,4,5,5-Tetramethyl-2-{3-oxabicyclo[4.1.0]heptan-6-yl}-1,3,2-dioxaborolane (Intermediate F)

From General Method A

A solution of 2-(3,6-dihydro-2H-pyran-4-yl)-4,4,5,5-tetramethyl-1,3,2-dioxaborolane (1050 mg, 5 mmol) in fluorobenzene (10 mL) was cooled to -5 °C and was treated slowly with diethylzinc in hexanes

(25.00 mL, 25.00 mmol) over 2 mins. The mixture was stirred at -5 °C for 5mins prior to treating with a solution of chloroiodomethane (8819 mg, 50.0 mmol) in fluorobenzene (5 ml) dropwise over 5min. The mixture was stirred at -5 °C for 10 min prior to three subsequent additions of diethylzinc and chloroiodomethane in the same manner. The reaction mixture was allowed to warm to room temperature and stirred for 16 h. The suspension was partitioned between aqueous NH_4Cl (75 ml) and diethyl ether (2 x 50 ml) and the dried over $MgSO_4$. The extract was evaporated onto florisil and purified by column chromatography to give 2-(3-oxabicyclo[4.1.0]heptan-6-yl)-4,4,5,5-tetramethyl-1,3,2-dioxaborolane (485 mg, 2.164 mmol, 43.3% yield).

^{1}H NMR (400 MHz, $CDCl_3$): δ ppm 4.02 (d, *J* = 11.25 Hz, 1H), 3.85 (dd, *J* = 3.42, 11.25 Hz, 1H), 3.61 (ddd, *J* = 2.45, 6.36, 11.25 Hz, 1H), 3.17 (dt, *J* = 4.89, 11.25 Hz, 1H), 2.00-2.08 (m, 1H), 1.62 -1.73 (m, 1H), 1.24 (s, 6H), 1.08 (br dd, *J* = 3.18, 5.62 Hz, 1H), 0.96 (dd, *J* = 2.93, 8.31 Hz, 1H), 0.66 (dd, *J* = 3.18, 5.62 Hz, 1H)

Potassium trifluoro({3-oxabicyclo[4.1.0]heptan-6-yl})boranuide (Intermediate G)

2-(3-oxabicyclo[4.1.0]heptan-6-yl)-4,4,5,5-tetramethyl-1,3,2-dioxaborolane (5 g, 22.31 mmol) was dissolved in anhydrous acetonitrile (55 mL) and anhydrous MeOH (55 mL) under a nitrogen atmosphere. Aqueous potassium fluoride (5.2 g, 90 mmol) in water (20 mL) was added and the suspension was stirred at room temperature under nitrogen for 10 minutes. (2*R*,3*R*)-2,3-dihydroxysuccinic acid (6.70 g, 44.6 mmol) was added followed by THF (2.5 mL). The reaction mixture was stirred for 1.25 h and left standing over night after which the precipitate filtered off and washed with acetonitrile. The filtrate was concentrated *in vacuo* and azeotroped with toluene (3 x 50 mL) and triturated with diethyl ether (3 x 30 mL) to give potassium trifluoro({3-oxabicyclo[4.1.0]heptan-6-yl})boranuide 4.83 g (106% yield).

^{1}H NMR (400 MHz, $CDCl_3$): δ ppm 4.02 (d, *J* = 11.25 Hz, 1H), 3.85 (dd, *J* = 3.42, 11.25 Hz, 1H), 3.61 (ddd, *J* = 2.45, 6.36, 11.25 Hz, 1H), 3.17 (dt, *J* = 4.89, 11.25 Hz, 1H), 1.86-2.11 (m, 1H), 1.58-1.85 (m, 1H), 1.20-1.29 (m, 9H), 1.03-1.16 (m, 1H), 0.96 (dd, *J* = 2.93, 8.31 Hz, 1H), 0.66 (dd, *J* = 3.18, 5.62 Hz, 1H)

2-Chloro-4-(3,6-dihydro-2H-pyran-4-yl)-6-(methanesulfonylmethyl)pyrimidine (Intermediate I)

From General Method A

Isolated as a mixture of 2,4-bis(3,6-dihydro-2H-pyran-4-yl)6((methylsulfonyl)methyl) pyrimidine with 2-chloro-4-(3,6-dihydro-2H-pyran-4-yl)-6-((methylsulfonyl)methyl)pyrimidine and used crude in the synthesis of compound **21**.

2-Chloro-4-(methanesulfonylmethyl)-6-{3-oxabicyclo[4.1.0]heptan-6-yl}pyrimidine (Intermediate J)

2,4-dichloro-6-((methylsulfonyl)methyl)pyrimidine (200 mg, 0.830 mmol), (3-oxabicyclo[4.1.0]heptan-6-yl)trifluoro-l4-borane, potassium salt (203 mg, 0.995 mmol), $PdCl_2$(dppf) (60.7 mg, 0.083 mmol) and caesium carbonate (541 mg, 1.659 mmol) were suspended in toluene (2000 µl) : water (200 µl) and the resulting mixture was degassed under a flow of nitrogen, sealed, and heated to 110 °C with stirring for 15 h. The reaction mixture was cooled to room temperature and treated with EtOAc (5 mL), the mixture was filtered through Celite and eluted with EtOAc (3 x 5 mL). The filtrate was evaporated *in vacuo* and purified by column chromatography (98.8 mg, 0.326 mmol, 39.3% yield). ^{1}H NMR (400MHz, $CDCl_3$): δ ppm 7.29 (s, 1H), 4.32 (s, 2H), 3.91 - 4.03 (m, 2H), 3.69 (ddd, 1H, J = 11.6 Hz, J = 5.7 Hz, J = 4.4 Hz), 3.42 (ddd, 1H, J = 11.7 Hz, J = 9.3 Hz, J = 5.1 Hz), 3.03 (s, 3H), 2.56 (dt, 1H, J = 13.9 Hz, J = 4.6 Hz), 2.09 (ddd, 1H, J = 14.2 Hz, J = 9.0 Hz, J = 5.9 Hz), 1.87 - 2.01 (m, 1H), 1.53 (dd, 1H, J = 9.2 Hz, J = 4.0 Hz), 1.33 (dd, 1H, J = 6.7 Hz, J = 4.3 Hz). ESI (m/z): $[M+H]^+$ = 303

Intermediate J was purified by chiral SFC for chiral separation to afford:

2-Chloro-4-(methanesulfonylmethyl)-6-[(1*S*, 6*R*)-3-oxabicyclo[4.1.0]heptan-6-yl]pyrimidine (Intermediate K)

^{1}H NMR (400 MHz, DMSO-d_6): δ ppm 7.61 (s, 1H), 4.68 (s, 2H), 3.78-3.97 (m, 2H), 3.55-3.62 (m, 1H), 3.32-3.41 (m, 1H), 3.11 (s, 3H), 2.44-2.57 (m, 1H), 1.96 (ddd, J = 5.70, 8.82, 14.20 Hz, 1H), 1.73-1.86 (m, 1H), 1.42 (dd, J = 3.95, 9.21 Hz, 1H), 1.25 (dd, J = 4.17, 6.80 Hz, 1H); ESI (m/z): $[M+H]^+$ = 303; $[\alpha]_D^{20}$ = -67

and

2-Chloro-4-(methanesulfonylmethyl)-6-[(1*R*,6*S*)-3-oxabicyclo[4.1.0]heptan-6-yl]pyrimidine (Intermediate L)

^{1}H NMR (400 MHz, DMSO-d_6): δ ppm 7.61 (s, 1H), 4.68 (s, 2H), 3.80-3.96 (m, 2H), 3.52-3.63 (m, 1H), 3.31-3.40 (m, 1H), 3.11 (s, 3H), 2.45-2.55 (m, 1H), 1.96 (ddd, *J* = 5.70, 8.82, 14.20 Hz, 1H), 1.73-1.86 (m, 1H), 1.42 (dd, *J* = 4.06, 9.32 Hz, 1H), 1.25 (dd, *J* = 4.17, 6.80 Hz, 1H); ESI (m/z): $[M+H]^+$ = 303; $[\alpha]_D^{20}$ 72

2-Chloro-4-(2-methanesulfonylpropan-2-yl)-6-{3-oxabicyclo[4.1.0]heptan-6-yl}pyrimidine (Intermediate M)

To a solution of 4-(3-oxabicyclo[4.1.0]heptan-6-yl)-2-chloro-6-((methylsulfonyl)methyl)pyrimidine (300 mg, 0.991 mmol) in anhydrous tetrahydrofuran (THF, 4 mL) was added sodium 2-methylpropan-2-olate 2M in THF (1.486 mL, 2.97 mmol) followed by dropwise addition of iodomethane (0.155 mL, 2.477 mmol). The resulting mixture was stirred at ambient temperature for 5 h. The reaction mixture was quenched with saturated ammonium chloride (10 mL) and extracted with DCM (2 x 10 mL). The organic phase was concentrated in vacuo and purified by column chromatography to afford 2-chloro-4-(2-methanesulfonylpropan-2-yl)-6-{3-oxabicyclo[4.1.0]heptan-6-yl}pyrimidine (328 mg, 0.985 mmol, 99% yield).

^{1}H NMR (400 MHz, $CDCl_3$): δ ppm 7.42 (s, 1H), 3.99 (d, *J* = 2.93 Hz, 2H), 3.70 (ddd, *J* = 4.40, 5.75, 11.62 Hz, 1H), 3.44 (ddd, *J* = 5.26, 9.23, 11.68 Hz, 1H), 2.91 (s, 3H), 2.56 (td, *J* = 4.86, 14.00 Hz, 1H), 2.05-2.19 (m, 2H), 1.92-1.99 (m, 1H), 1.84-1.89 (m, 7H), 1.48-1.55 (m, 1H), 1.25-1.36 (m, 2H); ESI (m/z): $[M+H]^+$ = 328

Intermediate M was purified by chiral SFC for chiral separation to afford:

2-Chloro-4-(2-methanesulfonylpropan-2-yl)-6-[(1*R*,6*S*)-3-oxabicyclo[4.1.0]heptan-6-yl]pyrimidine (Intermediate N)

^{1}H NMR (400 MHz, $CDCl_3$): δ ppm 7.42 (s, 1H), 3.99 (d, *J* = 2.69 Hz, 2H), 3.70 (ddd, *J* = 4.40, 5.87, 11.74 Hz, 1H), 3.44 (ddd, *J* = 5.14, 9.29, 11.74 Hz, 1H), 2.91 (s, 3H), 2.56 (td, *J* = 4.71, 14.06 Hz, 1H),

2.12 (ddd, *J* = 5.87, 8.93, 14.31 Hz, 1H), 1.95 (br d, *J* = 2.69 Hz, 1H), 1.87 (s, 6H), 1.52 (dd, *J* = 4.16, 9.29 Hz, 1H), 1.32 (dd, *J* = 4.28, 6.72 Hz, 1H); ESI (m/z): $[M+H]^+$ = 331; $[\alpha]_D^{20}$ = -72

and

2-Chloro-4-(2-methanesulfonylpropan-2-yl)-6-[(1*S*,6*R*)-3-oxabicyclo[4.1.0]heptan-6-yl]pyrimidine (Intermediate O)

Yield 66%. ^{1}H NMR (400 MHz, $CDCl_3$): δ ppm 7.42 (s, 1H), 3.99 (d, *J* = 2.69 Hz, 2H), 3.70 (ddd, *J* = 4.40, 5.87, 11.74 Hz, 1H), 3.44 (ddd, *J* = 5.26, 9.23, 11.68 Hz, 1H), 2.91 (s, 3H), 2.56 (td, *J* = 4.77, 13.94 Hz, 1H), 2.12 (ddd, *J* = 5.87, 8.99, 14.24 Hz, 1H), 1.95 (br d, *J* = 2.69 Hz, 1H), 1.87 (s, 6H), 1.52 (dd, *J* = 4.16, 9.29 Hz, 1H), 1.32 (dd, *J* = 4.28, 6.72 Hz, 1H). ESI (m/z): $[M+H]^+$ = 331. $[\alpha]_D^{20}$ = 78

4-[4-(2-Methanesulfonylpropan-2-yl)-6-[(1*R*,6*S*)-3-oxabicyclo[4.1.0]heptan-6-yl]pyrimidin-2-yl]aniline (Intermediate P)

From Intermediate N, General Method A

Yield 43%. ^{1}H NMR (400 MHz, DMSO-d_6): δ ppm 7.99-8.20 (d, *J* = 8.80 Hz, 2H), 7.25 (s, 1H), 6.63 (d, *J* = 8.80 Hz, 2H), 5.65 (s, 2H), 3.79-4.04 (m, 2H), 3.51-3.71 (m, 1H), 3.38 (ddd, *J* = 5.26, 8.77, 11.62 Hz, 1H), 2.97 (s, 3H), 2.61-2.77 (dt, *J* = 5.12, 14.09 Hz,1H), 2.00 (ddd, *J* = 5.59, 8.60, 14.09 Hz, 1H), 1.88-1.95 (m, 1H), 1.45 (dd, *J* = 3.73, 9.21 Hz, 1H), 1.15 (dd, *J* = 3.84, 6.47 Hz, 1H); ESI (m/z): $[M+H]^+$ = 388; $[\alpha]_D^{20}$ = -78

4-[4-(2-Methanesulfonylpropan-2-yl)-6-[(1*S*,6*R*)-3-oxabicyclo[4.1.0]heptan-6-yl]pyrimidin-2-yl]aniline (Intermediate Q)

From Intermediate O, General Method A

Yield 47%. ^{1}H NMR (400 MHz, DMSO-d_6): δ ppm 8.04-8.18 (d, *J* = 8.80 Hz,, 2H), 7.25 (s, 1H), 6.63 (d, *J* = 8.80 Hz, 2H), 5.65 (s, 2H), 3.78-4.01 (m, 2H), 3.53-3.65 (m, 1H), 3.38 (ddd, *J* = 5.15, 8.66, 11.62 Hz, 1H), 2.97 (s, 3H), 2.66 (td, *J* = 4.96, 13.98 Hz, 1H), 2.00 (ddd, *J* = 5.59, 8.66, 14.03 Hz, 1H), 1.87-1.95 (m, 1H), 1.45 (dd, *J* = 3.73, 9.21 Hz, 1H), 1.15 (dd, *J* = 3.84, 6.47 Hz, 1H); ESI (m/z): $[M+H]^+$ = 388; $[\alpha]_D^{20}$ = 67

3-[4-(3,6-Dihydro-2H-pyran-4-yl)pyrimidin-2-yl]phenol (9)

From Intermediate C, General method A

Yield 67%. ^{1}H NMR ($CDCl_3$, 400 MHz): δ ppm 8.74 (d, *J* = 5.4 Hz, 1H), 8.07 (dt, *J* = 7.8, 1.2 Hz, 1H), 8.00 (dd, *J* = 2.4, 1.5 Hz, 1H), 7.37 (t, *J* = 7.9 Hz, 1H), 7.22 (d, *J* = 5.4 Hz, 1H), 7.08 (dt, *J* = 2.9, 1.5 Hz, 1H), 7.00 (ddd, *J* = 8.1, 2.6, 0.9 Hz, 1H), 5.95-6.59 (m, 1H), 4.46 (q, *J* = 2.7 Hz, 2H), 4.00 (t, *J* = 5.5 Hz, 2H), 2.67-2.74 (m, 2H); ^{13}C NMR (101 MHz, $CDCl_3$): δ ppm 163.6, 163.3, 157.4, 156.2, 139.3, 133.1, 130.4, 129.9, 120.6, 118.0, 115.0, 113.2, 65.8, 64.3, 25.1; HRMS-ESI (m/z): calcd for $C_{15}H_{15}N_2O_2$, 255.1133; found $[M+H]^+$ 255.1121

3-(4-{3-Oxabicyclo[4.1.0]heptan-6-yl}pyrimidin-2-yl)phenol (12)

From Compound 7, General Method C

Yield 17%. ^{1}H NMR (400 MHz, $CDCl_3$): δ ppm 8.66 (d, *J* = 5.56 Hz, 1H), 8.03 (d, *J* = 7.83 Hz, 1H), 7.90-7.96 (m, 1H), 7.37 (t, *J* = 7.96 Hz, 1H), 7.11 (d, *J* = 5.56 Hz, 1H), 6.98 (dd, *J* = 2.27, 7.58 Hz, 1H), 4.05 (d, *J* = 2.78 Hz, 2H), 3.67-3.81 (m, 1H), 3.50 (ddd, *J* = 5.05, 9.09, 11.62 Hz, 1H), 2.71 (td, *J* = 4.80, 13.89 Hz, 1H), 2.15 (ddd, *J* = 5.68, 8.91, 14.21 Hz, 1H), 1.99 (tdd, *J* = 2.91, 6.22, 9.19 Hz, 1H), 1.56 (dd, *J* = 4.04, 9.35 Hz, 1H), 1.26 (dd, *J* = 4.04, 6.57 Hz, 1H); ^{13}C NMR (101 MHz, $CDCl_3$): δ ppm 173.2, 163.3, 156.6, 156.0, 139.4, 129.8, 120.6, 117.8, 114.8, 114.2, 65.6, 64.0, 25.2, 23.2, 23.1, 22; HRMS-ESI (m/z): calcd for $C_{16}H_{17}N_2O_2$, 269.1290; found $[M+H]^+$ 269.1276

The two enantiomers were separated by chiral HPLC on Chiralpak IC 250x20mm eluting with Heptane:EtOH: Isopropylamine 90:10:0.2 to give 3-{4-[(1*R*,6*S*)-3-oxabicyclo[4.1.0] heptan-6-yl]pyrimidin-2-yl}phenol **(12a)** $[\alpha]_D^{20}$ = -100 and 3-{4-[(1*S*,6*R*)-3-oxabicyclo[4.1.0] heptan-6-yl]pyrimidin-2-yl}phenol **(12b)** $[\alpha]_D^{20}$ = 70

3-(2-Hydroxyethyl)-1-{4-[4-(2-methanesulfonylpropan-2-yl)-6-[(1*S*,6*R*)-3-oxabicyclo[4.1.0] heptan-6-yl]pyrimidin-2-yl]phenylthiourea (29b)

From Intermediate P, General Method D

Yield 73%. ^{1}H NMR (600 MHz, DMSO-d_6): δ ppm 9.75-9.97 (m, 1H), 8.35 (d, J = 8.80 Hz, 2H), 7.91 (br s, 1H), 7.69 (d, J = 8.80 Hz, 2H), 4.82 (br s, 1H), 3.92-3.99 (m, 1H), 3.84-3.91 (m, 1H), 3.54-3.67 (m, 4H), 3.41 (ddd, J = 5.32, 8.71, 11.65 Hz, 1H), 2.99 (s, 3H), 2.71 (td, J = 4.95, 13.94 Hz, 1H), 1.93-2.09 (m, 2H), 1.84 (s, 6H), 1.52 (dd, J = 4.03, 9.17 Hz, 1H), 1.21 (dd, J = 4.03, 6.24 Hz, 1H); ^{13}C NMR (151 MHz, DMSO-d_6): δ ppm 180.7, 174.3, 166.1, 162.0, 142.6, 132.6, 128.8, 122.2, 122.1, 113.1, 67.0, 65.1, 63.5, 59.6, 47.0, 36.5, 25.1, 23.5, 23.4, 22.8, 21.0; HRMS-ESI (m/z): calcd for $C_{23}H_{31}N_4O_4S_2$, 491.1787; found $[M+H]^+$ 491.1787; $[\alpha]_D^{20}$ = 42

Acknowledgements

The authors would like to thank Alan Kennedy, Department of Pure and Applied Chemistry, University of Strathclyde, 295 Cathedral Street Glasgow, G1 1XL, U.K. for the small molecule crystal structure of **12b**.

Abbreviations used

mTOR, mammalian target of rapamycin; mTORC1, mTOR complex1; mTORC2, mTOR complex 2; PI3K, Phosphoinositide 3-kinase; PIKK, Phosphatidylinositol 3-kinase-related kinases; AKT, Protein Kinase B; MOE, Molecular Operating Environment; TFA, trifluoracetic acid; EtOAc, ethyl acetate; THF, tetrahydrofuran; DIPEA, diisopropylethylamine; DCM, dichloromethane; MeOH, Methanol; DMSO, dimethylsulphoxide; MS, mass spectroscopy; HPLC, high pressure liquid chromatography.

Ancillary Information

Included in the supporting information are:

Molecular formular strings; data for the small molecule crystal structure of 9b; a low occupancy co-crystal structure of **12b**; protocols for the PI3K, mTOR and Akt assays and experimental data for the remaining novel compounds **5** to **29** inclusive.

Contact emails: heather.x.hobbs@gsk.com; Gianpaolo.Bravi@dotmatics.com; ianb22@talktalk.net; maire.a.convery@gsk.com; hannah.r.davies@gsk.com; graham.g.inglis@gsk.com;

sandeep.8.pal@gsk.com; simon.2.peace@gsk.com; joanna.m.redmond@gsk.com and dec.summers92@gmail.com

References

1. Yap, T. A.; Garrett, M. D.; Walton, M. I.; Raynaud, F.; de Bono, J. S.; Workman, P. Targeting the PI3K–AKT–mTOR pathway: progress, pitfalls, and promises. *Curr. Opin. Pharmacol.* **2008,** 8, 393-412.
2. Liu, P.; Cheng, H.; Roberts, T. M.; Zhao, J. J. Targeting the phosphoinositide 3-kinase pathway in cancer. *Nat. Rev. Drug Discov.* **2009,** 8, 627 - 644.
3. Janku, F.; Yap, T. A.; Meric-Bernstam, F. Targeting the PI3K pathway in cancer: are we making headway? *Nat. Rev. Clin. Oncol.* **2018,** 15, 273-291.
4. Regad, T. Targeting RTK signaling pathways in cancer. *Cancers* **2015,** 7, 1758-1784.
5. Fritsche, L.; Weigert, C.; Haring, H.-U.; Lehmann, R. How insulin receptor substrate proteins regulate the metabolic capacity of the liver - implications for health and disease. *Curr. Med. Chem.* **2008,** 15, 1316-1329.
6. Heras-Sandoval, D.; Avila-Muñoz, E.; Arias, C. The phosphatidylinositol 3-kinase/mTor pathway as a therapeutic target for brain aging and neurodegeneration. *Pharmaceuticals* **2011,** 4, 1070-1087.
7. Heras-Sandoval, D.; Pérez-Rojas, J. M.; Hernández-Damián, J.; Pedraza-Chaverri, J. The role of PI3K/AKT/mTOR pathway in the modulation of autophagy and the clearance of protein aggregates in neurodegeneration. *Cell. Signal.* **2014,** 26, 2694-2701.
8. Wong, R. H. F.; Sul, H. S. Insulin signaling in fatty acid and fat synthesis: a transcriptional perspective. *Curr. Opin. Pharmacol.* **2010,** 10, 684-691.
9. Xu, J.; Wang, P.; Yang, H.; Zhou, J.; Li, Y.; Li, X.; Xue, W.; Yu, C.; Tian, Y.; Zhu, F. Comparison of FDA approved kinase targets to clinical trial ones: Insights from their system profiles and drug-target interaction networks. *Biomed. Res. Int.* **2016,** 2016, 1-9.
10. Janku, F. Phosphoinositide 3-kinase (PI3K) pathway inhibitors in solid tumors: From laboratory to patients. *Cancer Treat. Rev.* **2017,** 59, 93-101.
11. Lynch, J. T.; Polanska, U. M.; Delpuech, O.; Hancox, U.; Trinidad, A. G.; Michopoulos, F.; Lenaghan, C.; McEwen, R.; Bradford, J.; Polanski, R.; Ellston, R.; Avivar-Valderas, A.; Pilling, J.; Staniszewska, A.; Cumberbatch, M.; Critchlow, S. E.; Cruzalegui, F.; Barry, S. T. Inhibiting PI3Kβ with AZD8186 regulates key metabolic pathways in PTEN-null tumors. *Clin. Cancer Res.* **2017,** 23, 7584-7595.
12. Amour, A.; Barton, N.; Cooper, A. W. J.; Inglis, G.; Jamieson, C.; Luscombe, C. N.; Morrell, J.; Peace, S.; Perez, D.; Rowland, P.; Tame, C.; Uddin, S.; Vitulli, G.; Wellaway, N. Evolution of a novel, orally bioavailable series of PI3Kδ inhibitors from an inhaled lead for the treatment of respiratory disease. *J. Med. Chem.* **2016,** 59, 7239-7251.
13. Amour, A.; Barton, N.; Cooper, A. W. J.; Inglis, G.; Jamieson, C.; Luscombe, C. N.; Morrell, J.; Peace, S.; Perez, D.; Rowland, P.; Tame, C. J.; Uddin, S.; Vitulli, G.; Wellaway, N. Correction to evolution of a novel, orally bioavailable series of PI3Kδ inhibitors from an inhaled lead for the treatment of respiratory disease. *J. Med. Chem.* **2016,** 59, 8148-8148.
14. Gonzalez-Lopez de Turiso, F.; Hao, X.; Shin, Y.; Bui, M.; Campuzano, I. D. G.; Cardozo, M.; Dunn, M. C.; Duquette, J.; Fisher, B.; Foti, R. S.; Henne, K.; He, X.; Hu, Y.-L.; Kelly, R. C.; Johnson, M. G.; Lucas, B. S.; McCarter, J.; McGee, L. R.; Medina, J. C.; Metz, D.; San Miguel, T.; Mohn, D.; Tran, T.; Vissinga, C.; Wannberg, S.; Whittington, D. A.; Whoriskey, J.; Yu, G.; Zalameda, L.; Zhang, X.; Cushing, T. D. Discovery and in vivo evaluation of the potent and selective PI3Kδ inhibitors 2-((1*S*)-1-((6-amino-5-cyano-4-pyrimidinyl)amino)ethyl)-6-fluoro-N-methyl-3-(2-pyridinyl)-4-quinolinecarboxamide (AM-

0687) and 2-((1*S*)-1-((6-amino-5-cyano-4-pyrimidinyl)amino)ethyl)-5-fluoro-N-methyl-3-(2-pyridinyl)-4-quinolinecarboxamide (AM-1430). *J. Med. Chem.* **2016,** 59, 7252-7267.

15. Heffron, T. The discovery and process chemistry development of GDC-0084, a brain penetrating inhibitor of PI3K and mTOR. *ACS symposium series* **2016,** 1239, 147-173.

16. Shin, Y.; Suchomel, J.; Cardozo, M.; Duquette, J.; He, X.; Henne, K.; Hu, Y.-L.; Kelly, R. C.; McCarter, J.; McGee, L. R.; Medina, J. C.; Metz, D.; San Miguel, T.; Mohn, D.; Tran, T.; Vissinga, C.; Wong, S.; Wannberg, S.; Whittington, D. A.; Whoriskey, J.; Yu, G.; Zalameda, L.; Zhang, X.; Cushing, T. D. Discovery, optimization, and in vivo evaluation of benzimidazole derivatives AM-8508 and AM-9635 as potent and selective PI3Kδ inhibitors. *J. Med. Chem.* **2016,** 59, 431-447.

17. Cahn, A.; Hamblin, J. N.; Begg, M.; Wilson, R.; Dunsire, L.; Sriskantharajah, S.; Montembault, M.; Leemereise, C. N.; Galinanes-Garcia, L.; Watz, H.; Kirsten, A. M.; Fuhr, R.; Hessel, E. M. Safety, pharmacokinetics and dose-response characteristics of GSK2269557, an inhaled PI3Kδ inhibitor under development for the treatment of COPD. *Pulm. Pharmacol. Ther.* **2017,** 46, 69-77.

18. Vlahos, C. J.; Matter, W. F.; Hui, K. Y.; Brown, R. F. A specific inhibitor of phosphatidylinositol 3-kinase, 2-(4-morpholinyl)-8-phenyl-4H-1-benzopyran-4-one (LY294002). *J. Biol. Chem.* **1994,** 269, 5241-5248.

19. Gharbi, Severine I.; Zvelebil, Marketa J.; Shuttleworth, Stephen J.; Hancox, T.; Saghir, N.; Timms, John F.; Waterfield, Michael D. Exploring the specificity of the PI3K family inhibitor LY294002. *Biochem. J.* **2007,** 404, 15-21.

20. Walker, E. H.; Pacold, M. E.; Perisic, O.; Stephens, L.; Hawkins, P. T.; Wymann, M. P.; Williams, R. L. Structural determinants of phosphoinositide 3-kinase inhibition by wortmannin, LY294002, quercetin, myricetin, and staurosporine. *Mol. Cell* **2000,** 6, 909-919.

21. Yang, H.; Rudge, D. G.; Koos, J. D.; Vaidialingam, B.; Yang, H. J.; Pavletich, N. P. mTOR kinase structure, mechanism and regulation. *Nature* **2013,** 497, 217-224.

22. Muth, F.; Günther, M.; Bauer, S. M.; Döring, E.; Fischer, S.; Maier, J.; Drückes, P.; Köppler, J.; Trappe, J.; Rothbauer, U.; Koch, P.; Laufer, S. A. Tetra-substituted pyridinylimidazoles as dual inhibitors of p38α mitogen-activated protein kinase and c-Jun N-terminal kinase 3 for potential treatment of neurodegenerative diseases. *J. Med. Chem.* **2015,** 58, 443-456.

23. Zhu, W.; Sun, C.; Xu, S.; Wu, C.; Wu, J.; Xu, M.; Zhao, H.; Chen, L.; Zeng, W.; Zheng, P. Design, synthesis, anticancer activity and docking studies of novel 4-morpholino-7,8-dihydro-5H-thiopyrano[4,3-d]pyrimidine derivatives as mTOR inhibitors. *Bioorg. Med. Chem.* **2014,** 22, 6746-6754.

24. K-C Liu, K.; Bailey, S.; M Dinh, D.; Lam, H.; Li, C.; A Wells, P.; Yin, M.-J.; Zou, A. Conformationally-restricted cyclic sulfones as potent and selective mTOR kinase inhibitors. *Bioorg. Med. Chem. Lett.* **2012,** 22, 5114-5117.

25. Bochevarov, A. D.; Harder, E.; Hughes, T. F.; Greenwood, J. R.; Braden, D. A.; Philipp, D. M.; Rinaldo, D.; Halls, M. D.; Zhang, J.; Friesner, R. A. Jaguar: A high-performance quantum chemistry software program with strengths in life and materials sciences. *Int. J. Quantum Chem.* **2013,** 113, 2110-2142.

26. Andrs, M.; Korabecny, J.; Jun, D.; Hodny, Z.; Bartek, J.; Kuca, K. Phosphatidylinositol 3-kinase (PI3K) and phosphatidylinositol 3-kinase-related kinase (PIKK) inhibitors: Importance of the morpholine ring. *J. Med. Chem.* **2015,** 58, 41-71.

27. Kaplan, J.; Verheijen, J. C.; Brooijmans, N.; Toral-Barza, L.; Hollander, I.; Yu, K.; Zask, A. Discovery of 3,6-dihydro-2H-pyran as a morpholine replacement in 6-aryl-1H-pyrazolo[3,4-d]pyrimidines and 2-arylthieno[3,2-d]pyrimidines: ATP-competitive inhibitors of the mammalian target of rapamycin (mTOR). *Bioorg. Med. Chem. Lett.* **2010,** 20, 640-643.

28. Ritchie, T. J.; Macdonald, S. J. F.; Young, R. J.; Pickett, S. D. The impact of aromatic ring count on compound developability: further insights by examining carbo- and hetero-aromatic and -aliphatic ring types. *Drug Discov. Today* **2011,** 16, 164-171.

29. Ritchie, T. J.; Macdonald, S. J. F. Physicochemical descriptors of aromatic character and their use in drug discovery. *J. Med. Chem.* **2014,** 57, 7206-7215.

30. Lovering, F.; Bikker, J.; Humblet, C. Escape from flatland: Increasing saturation as an approach to improving clinical success. *J. Med. Chem.* **2009,** 52, 6752-6756.
31. Lovering, F. Escape from Flatland 2: complexity and promiscuity. *Med. Chem. Comm.* **2013,** 4, 515-519.
32. Collins, C. J. Protonated cyclopropanes. *Chem. Rev.* **1969,** 69, 543-550.
33. Dorko, E. A.; Hencher, J. L.; Bauer, S. H. The molecular structure of trimethylenecyclopropane. *Tetrahedron* **1968,** 24, 2425-2434.
34. Armin, d. M. Bonding properties of cyclopropane and their chemical consequences. *Angew. Chem. Int. Edit.* **1979,** 18, 809-826.
35. Chemical Computing Group., U. Molecular operating environment (MOE). In 1010 Sherbooke St. West, Suite #910, Montreal, QC, Canada, H3A 2R7,, 2019.
36. Convery, M. H. H. K. A. P. S. P. S. P. P. S., D.; Jamieson C. A theoretical and experimental investigation into the conformational bias of aryl cyclopropylpyrans, novel biosteres for N-aryl morpholines. *Manuscript in perparation* **2018**.
37. Smerdon, S. J. A year in structural signaling: mTOR—The PIKK of the bunch? *Sci. Signal.* **2014,** 7, pe6-pe6.
38. Cornu, M.; Albert, V.; Hall, M. N. mTOR in aging, metabolism, and cancer. *Curr. Opin. Genet. Dev.* **2013,** 23, 53-62.
39. Zoncu, R.; Efeyan, A.; Sabatini, D. M. mTOR: from growth signal integration to cancer, diabetes and ageing. *Nat. Rev. Mol. Cell Bio.* **2010,** 12, 21-35.
40. Lawrence, J.; Nho, R. The role of the mammalian target of rapamycin (mTOR) in pulmonary fibrosis. *Int. J. Mol. Sci.* **2018,** 19, 778.
41. Holroyd, A. K.; Michie, A. M. The role of mTOR-mediated signaling in the regulation of cellular migration. *Immunol. Lett.* **2018,** 196, 74-79.
42. Hazel, Q.; Chieh, L. Y.; F, L. M.; L, R. T. PIKKing a way to regulate inflammation. *Immunol. Cell Biol.* **2018,** 96, 8-20.
43. Sabatini, D. M. Twenty-five years of mTOR: Uncovering the link from nutrients to growth. *Proc. Nat. Acad. Sci.* **2017,** 114, 11818-11825.
44. Pike, K. G.; Morris, J.; Ruston, L.; Pass, S. L.; Greenwood, R.; Williams, E. J.; Demeritt, J.; Culshaw, J. D.; Gill, K.; Pass, M.; Finlay, M. R. V.; Good, C. J.; Roberts, C. A.; Currie, G. S.; Blades, K.; Eden, J. M.; Pearson, S. E. Discovery of AZD3147: A potent, selective dual inhibitor of mTORC1 and mTORC2. *J. Med. Chem.* **2015,** 58, 2326-2349.
45. Foote, K. M.; Blades, K.; Cronin, A.; Fillery, S.; Guichard, S. S.; Hassall, L.; Hickson, I.; Jacq, X.; Jewsbury, P. J.; McGuire, T. M.; Nissink, J. W. M.; Odedra, R.; Page, K.; Perkins, P.; Suleman, A.; Tam, K.; Thommes, P.; Broadhurst, R.; Wood, C. Discovery of 4-{4-[(3R)-3-methylmorpholin-4-yl]-6-[1-(methylsulfonyl)cyclopropyl]pyrimidin-2-yl}-1H-indole (AZ20): A potent and selective inhibitor of ATR protein kinase with monotherapy in vivo antitumor activity. *J. Med. Chem.* **2013,** 56, 2125-2138.
46. Miyaura, N.; Yamada, K.; Suzuki, A. A new stereospecific cross-coupling by the palladium-catalyzed reaction of 1-alkenylboranes with 1-alkenyl or 1-alkynyl halides. *Tetrahedron Lett.* **1979,** 20, 3437-3440.
47. Gujral, S.; Khatri, S.; Riyal, P. Suzuki cross coupling reaction-a review. *Indo Glob. J. Pharm. Sci* **2012,** 2, 351-367.

Table of Contents graphic:

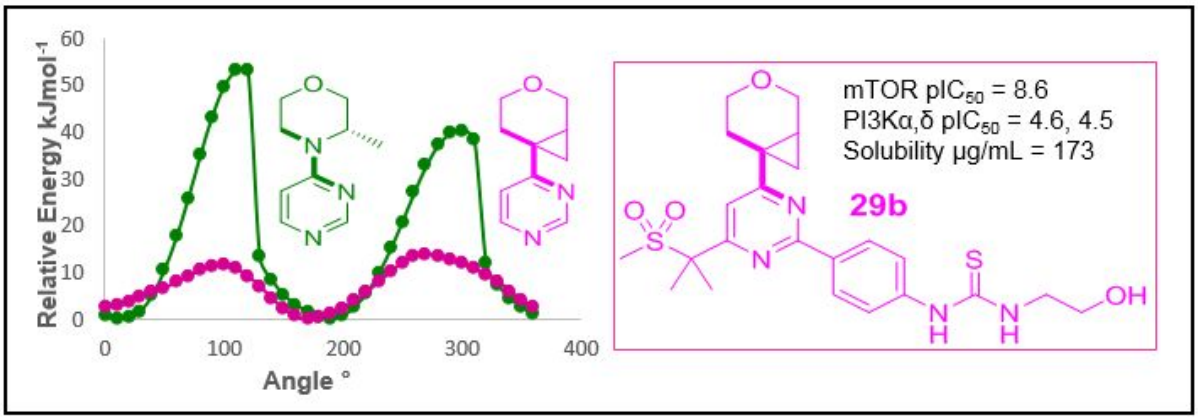
Relative Energy kJmol-1
60
50
40
30
20
10
0
0
100
200
300
400
Angle °
mTOR pIC50 = 8.6
PI3Kα,δ pIC50 = 4.6, 4.5
Solubility µg/mL = 173
29b

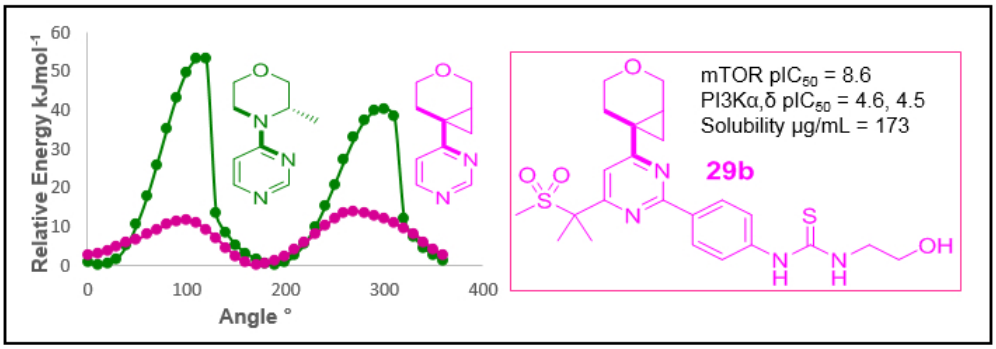

Energy minimised structure of 29b, a 3-oxabicyclo[4.1.0]heptane nanomolar mTOR inhibitor

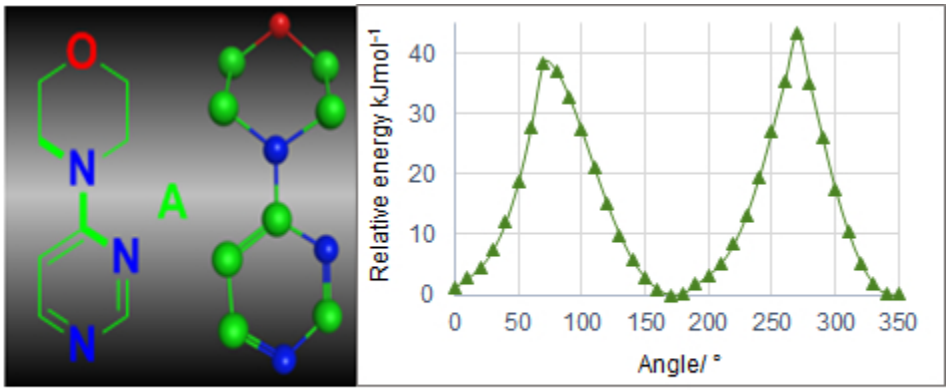

Figure 2: Energy minimised structure using MMFF94X forcefield in in MOE and dihedral scanning plot of 4-(Pyrimidin-4-yl)morpholine **A**

Figure 2: (a) Energy minimised structure of 4-(Pyrimidin-4-yl)morpholine A using DFT. (b) Energy scanning plot of CNcn dihedral bond angle of A

124x62mm (96 x 96 DPI)

Figure 3: Dihydropyran pyrimidine [B], Tetrahydropyran pyrimidine [C] & CPP pyrimidine [D] Energy minimised structures using MMFF94X forcefield in MOE

Figure 3: Dihydropyran pyrimidine [B], Tetrahydropyran pyrimidine [C] & CPP pyrimidine [D] Energy minimised structures using MMFF94X forcefield in MOE

151x60mm (96 x 96 DPI)

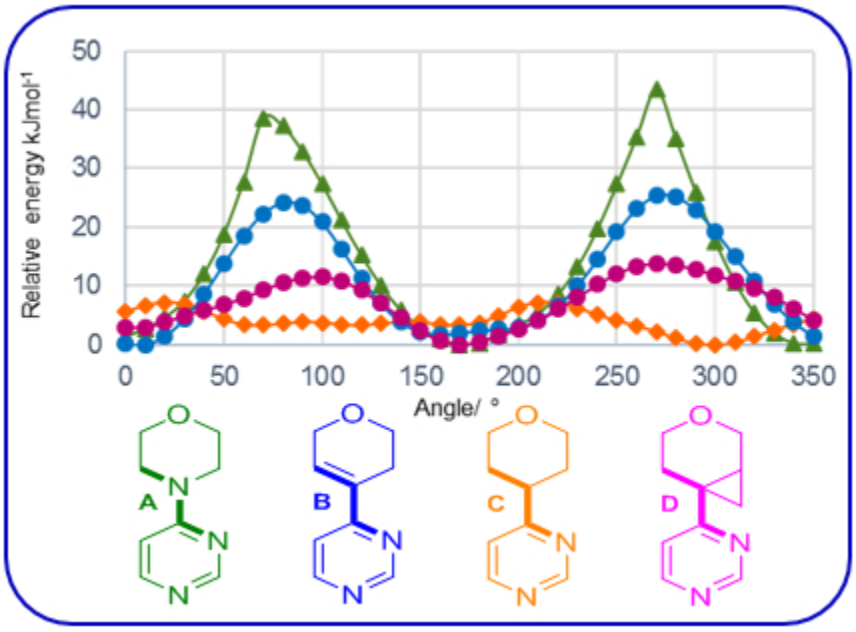

Figure 4: Dihedral scanning plots for various pyrimidine fragments using DFT/6-31G**

116x84mm (96 x 96 DPI)

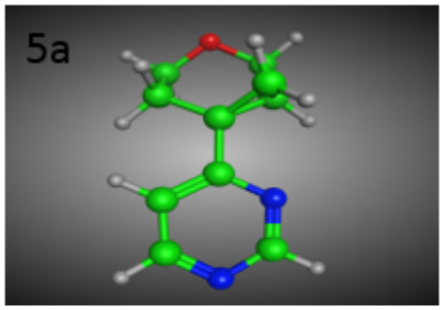

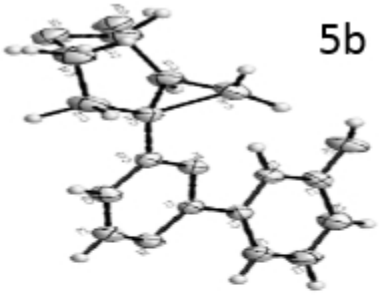

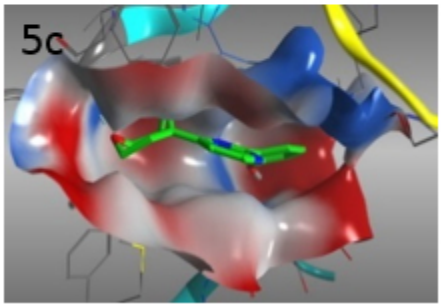

Figure 5a: QM predicted structure using DFT/6-31G**
5b: small molecule crystal structure of **12b** (CCDC 1864315 -See supplementary information)
5c: A potential binding mode of **12b** which is consistent with a low occupancy co-crystal structure in PI3Kδ (not deposited).